2 of 3

MECHANICAL

TECHNOLOGY

INCORPORATED

71 p $3.00 hc
$0.75 mf

U. S. NAVY
MARINE ENGINEERING LABORATORY
ANNAPOLIS, MARYLAND 21402

Contract Research Conducted for

U. S. Navy
Marine Engineering Laboratory

MEL Report 141/64

MTI 64TR22

PRELIMINARY ANALYTICAL INVESTIGATION OF RADIAL FACE SEALS

by

F. K. Orcutt
H. S. Cheng

April 24, 1964

Mechanical Technology Incorporated
968 Albany-Shaker Road
Latham, New York

MTI 64TR22

PRELIMINARY ANALYTICAL INVESTIGATION OF RADIAL FACE SEALS

by

F. K. Orcutt
H. S. Cheng

April 24, 1964

TECHNICAL REPORT

No. MTI 64TR22
Date April 24, 1964

PRELIMINARY ANALYTICAL INVESTIGATION OF RADIAL FACE SEALS

by

F. K. Orcutt
H. S. Cheng

F. K. Orcutt H. S. Cheng
Author(s)

Approved by

Approved by

Prepared for

U. S. Navy Marine Engineering Laboratory
Annapolis, Maryland

Prepared under

Contract N 161-25688

MECHANICAL TECHNOLOGY INCORPORATED
LATHAM, N.Y.

TABLE OF CONTENTS

INTRODUCTION

A key problem area in the development of very deep submergence submarines is to devise effective, reliable means of sealing propellor shafts. Seals for this service will require capabilities well beyond those of the propellor shaft seals in current service. The needed improvements in performance may be obtainable through refinement of the present sealing concept, the pressure balanced face seal, or it may be necessary to resort to some new sealing concept. Before embarking on a large scale search for new sealing concepts which hopefully have some fundamental advantage over the face seal, it is reasonable first to perform some theoretical and experimental analysis of face seals. The aim of these studies should be to point the way for worthwhile improvements in face seal capabilities or, alternatively, to show that there are fundamental limitations inherent in this concept which will probably negate efforts to effect really substantial further improvements.

This report is the product of a preliminary study of the problem which had as its major purpose to define a comprehensive program of analysis which should accomplish the objectives described above. The major phases of this preliminary study which are covered in this report are:

a) A critical review of the literature on fundamental principles of face seal performance.

b) Development of approximate methods for analyzing face seal performance to indicate which physical processes are most important and, in a qualitative way at least, to show how these processes can be controlled.

c) Application of the analyses which have been devised to seals which are representative of deep submergence submarine propellor shaft seals.

REVIEW OF FACE SEAL FUNDAMENTALS LITERATURE

The state of the technology of shaft sealing is clearly revealed by a review of the published literature. There are numerous papers describing empirically derived, qualitative recommendations for coping with problems which may arise in various applications. These are of little interest to this investigation. There are some papers describing more fundamental studies of seal behavior, but it is very clear that there is no developed, complete theory of seal operation comparable to say, fluid film bearing theory. The problem is that there is no clear identification of the physical processes which control face seal lubrication, leakage and wear. Consequently, the work which has been done on face seal fundamentals has generally considered a limited aspect of the problem and frequently assumes that certain conditions exist and then goes on to show what the consequences of these assumed conditions are. With few exceptions, there has been no serious effort to show that the assumed conditions must exist and be perpetuated because of the very nature of the seal and the conditions imposed on it. The idealized face seal has perfectly flat, smooth faces which have only circumferential relative motion, and the features of the seal which govern its performance are evidently unplanned deviations from these idealized conditions. It is difficult to devise a broadly applicable, quantitative theory of seal operation based on seal features which are not planned or controlled by the designer or user. However, some worthwhile contributions have been made toward development of a qualitative theory of face seal operation. These may be divided into papers describing analyses of seal lubrication, pressure induced deformation, effects of interfacial film geometry and fundamental experimental studies.

Seal Lubrication

There have been a number of seal or parallel surface thrust bearing lubrication analyses in which the hydrodynamic effects arising from one of a number of types of unplanned motions or deviations from surface flatness are determined. These analyses show that substantial load carrying capacity may be developed from virtually any of the suggested motions or deformations, providing it is assumed that subambient pressures will not be permitted to occur because of film rupture. Contributions of this type for different types of motions and deformations include those of Iny and Cameron[1], Whiteman[2], Nahavandi and Osterle[3], Tanner[4] and

Saibel and Lyman[5]. The principal criticism of all of these papers is that they begin with some assumed geometry or amplitude of motion which may be reasonable enough but which is not planned. They make no real effort to show that such a condition will exist in reality, or especially, that it must exist because of some self-perpetuating mechanism such as the elastohydrodynamic of thermal-hydrodynamic effect. The boundary condition for film rupture used in these analyses was to set the cut-off pressure at the ambient, low pressure condition. This is the usual procedure in bearing theory and it is appropriate for flat surface thrust bearings or unpressurized seals also. However, some other treatment appears to be needed for the case of highly pressurized seals when the liquid can be expected to be saturated with gas at the high pressure. Film rupture due to gas evolution could be expected at higher than ambient pressures for both hydrodynamic and hydrostatic pressure flows under these circumstances. The effects on interfacial pressure distribution would be in the direction of higher load capacity and they could well be significant.

Pressure Induced Deformation of the Primary Elements

The paper by Nau and Turnbull[6] is a valuable contribution in this area. The only form of deformation considered is the uneven axial compression of the low mudulus element due to the radial variation in film pressure across the seal face. The analysis is unique among face seal theories to date in that the elasticity and fluid flow equations are solved in coupled form. The results show how the net hydrostatic force balance will vary with pressure because of the deformation. A seal with a net positive hydraulic pressure balance (faces held together under load) at low-sealed fluid pressures when the radial pressure distribution is nearly linear may have complete separation of the faces even without rotation at high pressures because of the shift in film pressure distribution caused by elastic deformation. The effect of varying the minimum film thickness is also examined, resulting in a calculated film spring rate for hydrostatic effects only. A simplified expression for elastic deformation was used in which the deformation is directly proportional to the pressure. This expression should be reasonably valid for element geometries of the seal ring type where the radial film boundaries coincide with the edges of the faces. It is not valid for cases where significant shear stresses will exist such as the typical, runner ring where the face surface extends beyond the film boundaries, or for high values of the deformation parameter (nigh values of pressure and low values of modulus). Also, its use in cases where the

low modulus seal ring is firmly held in a retaining ring of high modulus material is not correct.

While analysis of this type is an essential part ofunderstanding high-pressure seal behavior, it is clearly not sufficient alone, for it neglects the effects of rotation completely and it is quite certain that face seal behavior is very much dependent on rotation. For example, leakage is normally much lower when the seal is stationary than it is with rotation. Starting torque is considerably higher than running torque and running torque is inversely related to speed of rotation.

The paper by Fisher[7] considers the effects of radial twisting of the seal ring type of primary element caused by the pressure difference from inside to outside of the seal ring. This effect may be important in some seals, but it appears that it can be controlled by proper design. Certainly it should be considered in high-pressure seal design, and the analysis set forth by Fisher can be profitably employed in design calculations.

Effects of Interfacial Film Geometry on Pressure Distribution

The most useful and comprehensive work in this area is that of Snapp[8]. From calculations of radial film pressure distribution for various types of interfacial film geometries, he shows that the net hydrostatic load on the seal will vary significantly, depending on the film geometry which will be influenced by pressure and thermally induced deformations, uneven wear and initial conditions. The effects of even small changes in radial film shape on the net force tending to hold the faces together can be very large in high-pressure seals with highly variable and severe demands on the seal lubrication processes if high wear or excessive leakage are to be avoided. The results presented in the paper are very instructive, but they would have been more broadly useful if they had been presented in dimensionless form through normalization of the variables.

Experimental Studies

Denny's[9] report is an excellent and highly instructive description of a series of fundamental experiments aimed at pointing out the important characteristic features of face seal behavior. Greater use of it should have been made by the theoretical investigators in establishing the geometries or motions assumed in their calculations and then, through a comparison of calculated and measured load capacities, an effort

could be made to obtain some verification of their theoretical results. Jagger[10] and Iny and Cameron[1] also present experimental data of more limited scope but perhaps greater sophistication, which is generally consistent with Denny's results. In all of these papers the sealed fluid pressures are quite low and there is a need for fundamental experiments aimed at revealing the special features of high pressure seals.

I. PRELIMINARY ANALYSIS OF FACE-SEAL PERFORMANCE

There is no straightforward approach to the analysis of face-seal lubrication and leakage which can promise clear cut, quantitative prediction of performance as there is for example for fluid film bearings operating within the normal range of conditions. Successful operation of face seals in difficult applications seems to depend largely on unplanned, uncontrolled features of seal behavior. To date, there is no clear identification of which of these features dominate seal performance. In these circumstances, the most profitable approach to face-seal analysis is to perform qualitative studies of limited scope for the purpose of evaluating the significance of the various effects which may be important. Following this procedure, it will be appropriate to perform more comprehensive and rigorous analysis considering the combined effects of the most important aspects of seal behavior and aimed at providing more precise quantitative results.

During this program, approximate analytical methods have been developed for investigation of the following aspects of face seal performance:

1. Analysis of film pressure for an arbitrary film shape including both radial and circumferential effects.

2. Approximate analysis of the elastic deformation of the primary seal elements caused by hydrostatic pressure effects and considering the effects of the seal ring support structure.

3. Approximate analysis for the temperature rise of the interfacial film and the seal elements and for thermal distortion.

4. Approximate analysis of the response of the seal to dynamic loading or vibration.

5. Estimate of the significance of elastohydrodynamic lubrication effects in seal performance.

6. Estimate of the significance of thermal-hydrodynamic lubrication effects in seal performance.

These methods of analysis are generally applicable to diagnostic studies of all types of face seals. However, since we are concerned here with deep submergence submarine propeller shaft seals the general seal configuration which is chosen as a basis for the analysis will be representative of that type of seal (Figure 1).

The seal ring is the non-rotating, flexibly mounted member and is made of a relatively low modulus material. Its retaining ring is of a high modulus material and relatively heavy cross section. The rotor is also of high modulus material and extremely heavy cross section. The high pressure sealed fluid is on the outside with ambient pressure on the inside.

Analysis of Pressure for an Arbitrary Film Shape

Elastic or thermal distortion or uneven wear may deform the seal ring and runner surfaces to form a converging or diverging section radially and a wavy shape circumferentially. The radial profile of the interfacial film will determine the distribution of hydrostatic pressure across the faces and circumferential waviness will influence hydrodynamic pressure generation in the film Therefore, a computer program has been prepared to calculate the film pressure, load capacity, leakage and torque of the seal for an arbitrary film shape so that the effects of various types and combinations of seal face deformations can be investigated.

For this calculation the well-known short bearing equation is used with appropriate boundary conditions. The development of the solution and the analytical expressions used to describe various types of film shape are discussed in more detail in Appendix A. The results are presented in dimensionless form with the load capacity represented as the ratio of the average pressure in the film to the sealed fluid pressure ($\bar{P}/P_o$). The hydrodynamic pressure parameter (comparable to the Sommerfield number in bearing analysis) is:

$$\Lambda = \frac{6\mu\omega}{p_o}\left(\frac{r_o - r_i}{\bar{h}_i}\right)^2$$

where

μ = viscosity of the fluid, $\frac{lb}{in^2}$/sec.

ω = rotational speed, rad/sec.

p_o = sealed fluid pressure, psig.

$\bar{h}_i$ = average circumferential film thickness at inner radius, in.

The system of coordinates used in the analysis is shown in Figure 2.

Results were obtained for the following three film shapes:

1. Linear Profile with a superimposed saddle shaped circumferential waviness.

The graphical representation of this film is shown below

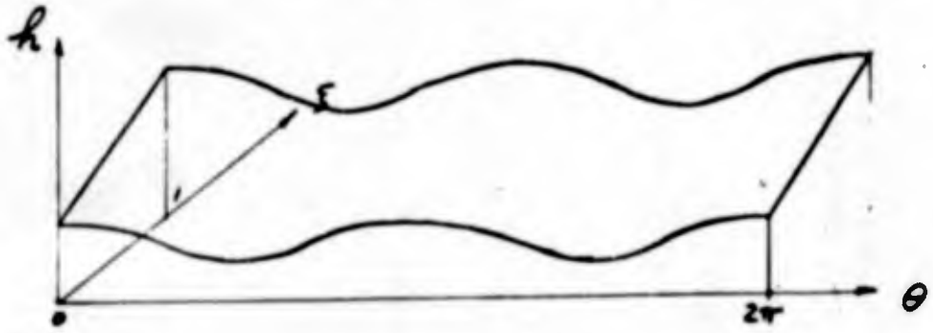

and it can be represented mathematically by

$$H = (1 + \lambda\xi) + \epsilon_2 \cos 2\theta$$

where λ measures the radial slope of the linear profile and ϵ_2 the circumferential waviness. It is noted that

λ is equal to $\frac{\bar{h}_o - \bar{h}_i}{\bar{h}_i}$, where $\bar{h}_o$ and $\bar{h}_i$

are the average circumferential maximum and minimum film thicknesses.

In figure 3, the ratio of the average face pressure to applied pressure is plotted against the variation of λ with ϵ_2 and Λ as parameters. The reason that Λ/λ^2 is chosen as parameter is because it does not involve the film thickness.
For cases of low $\frac{\Lambda}{\lambda^2}$ and slight circumferential waviness, the hydrodynamic action creates a circumferential pressure fluctuation but does not contribute to any increase in total load. When either $\frac{\Lambda}{\lambda^2}$ or ϵ_2 increases the subambient pressure appears in the film and since these subambient pressures are disallowed, there is an increase in load capacity as shown in the curves for high ϵ_2 and high $\frac{\Lambda}{\lambda^2}$.

2. A convergent profile based on the Nau-Turnbull solution (6) coupled with a saddled-shaped circumferential waviness.

The mathematical representation of this profile is:

$$H = \left\{(1+\lambda)^4 + (1-\xi)\left[1-(1+\lambda)^4\right]\right\}^{1/4} + \varepsilon_2 \cos 2\theta$$

The load capacity curves for the Nau-Turnbull profile are shown in Fig. 4. Similar trends exist between these curves and those for the linear profile. It is interesting to note that for high values of λ, the linear profile shows a higher load capacity than that calculated from the Nau-Turnbull profile.

However, the validity of Nau-Turnbill's solution for high values of is certainly questionable since high shear stresses are likely to be associated with the sharp pressure gradient at the end of the minimum film.

3. Snapp (8) reported an interesting case for a symmetrical parabolic radial profile and he showed that load capacity for this profile is the same as that for a parallel profile.

If a symmetrical wear pattern occurs both at inlet and outlet side, then a profile similar to a symmetrical parabolic type certainly would prevail. However, if the elastic deformation is superimposed on the wear profile, it is likely the radial profile during operation will be one similar to a non-symmetrical parabolic profile. Figure 5 shows the load capacity curve for such a profile without the circumferential waviness. Figure 6 shows a radial pressure distribution for this profile. Such a profile can be mathematically represented by -

$$H = \left[1 + \xi C + C(2\xi - 1)^2\right] \frac{1}{(1+C)} \qquad \text{for} \quad 0 < \xi < 1$$

The constant c, can be adjusted to obtain various values for $\frac{\bar{h}_{max} - \bar{h}_{min}}{\bar{h}_{min}}$.

As λ approaches infinity, the load capacity for this profile decreases gradually and approaches an asymtolic and is equal to ξ_m, (ξ_m is the value of ξ at the minimum film). This implies that if wear creates a convergent and divergent profile such as the non-symmetric parabolic profile, it would require a much lower minimum film thickness to support the same load compared to all converging profiles.

Estimate of Elastic Deformations

The accurate determination of elastic deformations in the rotor and the seal due to hydrostatic and hydrodynamic pressures is a very complex elasticity problem. Since the primary objective of this report is to seek an order of magnitude of these deformations, major simplifications have been made wherever possible in order to use the existing simple theories to estimate the deformation.

A typical seal subjected to an arbitrarily distributed pressure is shown below

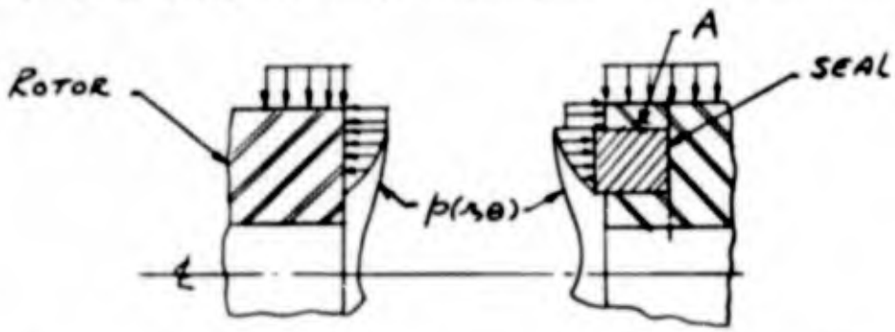

Since the rotor and the backing ring of the seal are made of short cylinders of heavy wall thickness and high modulus material, the deformation due to bending is assumed to be small and is not included in the estimate with the exception of a small section A adjacent to the seal ring as shown in the above figure. The normal deformation in the rotor due to the normal pressure acting on the face is calculated by using the classical elastic half-space solution. This is done in Appendix B. The results indicate that elastic deformation of the rotor can be considered negligible in comparison with deformation of the seal ring.

Calculation of the elastic deformation of the seal ring is considerably more involved because the effects of the backing ring must be considered. Normal deformation of the seal ring due to interfacial pressure will depend to a large extent on the ability of the boundary between seal ring and backing ring to sustain shear. Also, radial deformation of the seal ring will depend to a large extent on the support given by the seal ring. The radial stiffness of the backing ring will be lower near the seal interface because its effective cross-section is reduced by the seal ring. Consequently a twisting or inward bellmouthing distortion of the seal ring face will be caused by high hydrostatic pressures. An accurate

determination of the distribution of normal displacement of the seal ring face in the radial direction requires either an axi-symmetrical or a two dimensional plain strain elasticity solution with realistic boundary conditions at the seal ring-retainer ring interfaces. However, an order of magnitude estimate of the surface deformation can be had by using the approach outlined in Appendix B.

Estimate of the Temperature Rise and Thermal Distortion

In order to estimate the temperature distribution and thermal distortion of the primary seal elements it is necessary to establish a heat flux distribution. This is done by assuming an initial film shape, average thickness and operating condition to determine a distribution of shear rate within the film. Then, the film temperature and the surface temperature of the seal elements are determined by conservative approximate analysis from the known shear rate distribution. The estimate of thermal deformation can be had from the seal temperature distribution and comparison with the assumed surface waviness will indicate the qualitative significance of the thermal effects.

In order to stay on the conservative side, the film temperature is evaluated by assuming that all heat generated from viscous action is carried away by convection. From this assumption, the film temperature can be written as

$$\Delta T_f = 1.75 \cdot 10^{-4} \left(\frac{\mu U^2 r_m}{\rho_f C Q} \right) \int_{r_1}^{r_2} \frac{dr}{h} \qquad (1)$$

where

ΔT_f	= temperature rise in the fluid	^{o}F
μ	= viscosity of the fluid	$\frac{lb}{in^2}$ sec.
U	= average tangential velocity	in/sec.
h	= film thickness	in
ρ_f	= density of the fluid	lb/in^3
C	= specific heat of the fluid	$B/^{o}F/lb$
Q	= leakage rate	gpm

The temperature distribution for a seal-rotor section as shown in Fig. 1 is calculated by assuming all heat to be conducted away through the seal. An available in-house computer problem for the two-dimensional heat conduction equation is used for this calculation.

Once the temperature distribution is known in the seal or rotor, the thermal displacement on the surface can be determined by assuming that the thermal strain in the axial direction is expressed as

$$(\epsilon_z)_t = \alpha T \tag{2}$$

It follows that the

$$\omega_t(r) = \int_0^{H_s} (\epsilon_z)_t \, dz = \alpha \int_0^{H_s} T(r,z) \, dz \tag{3}$$

Dynamic Response of the Seal To Rotor Oscillation

Vibration of the seal faces, described as wobble or bounce, has been advanced as a possible mechanism for hydrodynamic load carrying capacity. A number of solutions for load carrying capacity for some assumed form of relative motion have been made. However, there was no effort made to show that relative motions of the order of magnitude of those which were assumed will exist in operating seals. Therefore, a simplified analysis was performed here to provide a means for estimating the dynamic response of the seal and therefore to evaluate the significance of vibration induced load support mechanisms.

A simplified one-dimensional vibration model for the seal and rotor system is shown below.

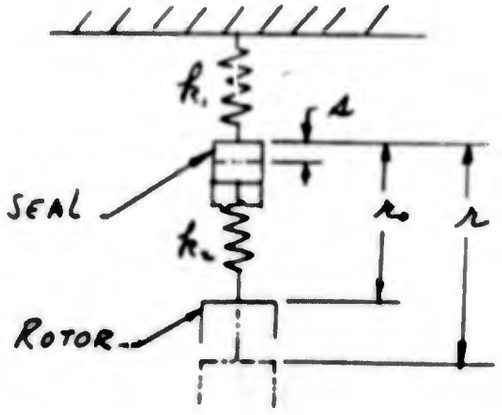

In this model, the mass of the seal is lumped at its center and the equivalent stiffnesses k_1 and k_2 are defined by

$$\frac{1}{k_1} = \frac{1}{k_s} + \frac{AE}{H_s} \tag{4}$$

$$\frac{1}{k_2} = \frac{1}{k_f} + \frac{AE}{H_s} \tag{5}$$

where k_s and k_f are the stiffness for the seal back-up springs and fluid film respectively. The term AE/H_s accounts for the elasticity of the seal itself. The equation of motion becomes

$$m\ddot{\rho} + c\dot{\rho} + (k_1 + k_2)\rho = (r - r_0)k_2 \tag{6}$$

where m and c are the mass of the seal and a combined viscous damping constant. The oscillation, $(r-r_o)$, can be broken down into Fourier Components which can be expressed by

$$f_n \cos n\omega t \tag{7}$$

Let A_n be the amplitude of the response to the oscillation f_n, then

$$A_n = \frac{f_n}{\left[\left(1 + \frac{k_1}{k_2} - \frac{n^2\omega^2 m}{k_2}\right)^2 + \left(\frac{n\omega c}{k_2}\right)^2\right]^{1/2}} \tag{8}$$

For normal operating conditions,

$$\begin{aligned} k_1 &\ll k_2 \\ n^2\omega^2 m &\ll k_2 \\ n\omega c &\ll k_2 \end{aligned} \tag{9}$$

Therefore, the seal should follow the rotor oscillations almost exactly and this implies that the axial vibration of the rotor should have very little effect upon the film shape between the seal elements.

Estimate of the Significance of Elastohydrodynamic Effects in the Circumferential Direction

Circumferential waviness of the seal faces may result in significant hydrodynamic load capacity under certain circumstances. A major difficulty in performing a rational analysis of this hydrodynamic effect or in attempting to control it has been the fact that wear should progressively alter and attenuate the waviness characteristic which initially exists. There are several effects which may tend to perpetuate or even reinforce an existing circumferential waviness in spite of wear. One of these is the elastohydrodynamic effect in which the hydrodynamic circumferential variation in film pressure caused by an initial surface waviness in turn causes elastic deformation of the surfaces normal to the film. A criterion has been developed to indicate when elastohydrodynamic effects should be significant. This is done by comparing the amplitude of an initial circumferential waviness with the amplitude of the resulting elastohydrodynamic deformation. When the deformation is equal to or greater than the original waviness, the elastohydrodynamic effect is significant. The criterion which is developed in Appendix C is:

$$\sigma_E = \frac{6\mu\omega}{8}\left(\frac{r_o - r_i}{\bar{h}_i}\right)^2 \frac{H_s}{\bar{h}_i E_s} \qquad (10)$$

$\sigma_E \geq 1$ EHD effects are significant

$\sigma_E \ll 1$ EHD effects are insignificant

Large value of axial thickness of the low modulus seal element (H_s) and small values of modulus of elasticity of this element (E_s) as well as high speed and sealed fluid viscosity tend to increase the importance of the elastohydrodynamic effect.

Estimate of the Significance of Thermal-Hydrodynamic Effects in the Circumferential Direction

The thermal-hydrodynamic effect is another possible means whereby an initial surface waviness may be perpetuated or reinforced. There will be a circumferential variation in shear rate and therefore in heat flux corresponding to the surface waviness. The heat flux and therefore the seal face temperature will be higher where the films are thinner and the resulting differences in local, normal expansion of the seal elements will reinforce the existing waviness. A criterion has been developed for estimating the importance of the thermal-hydrodynamic effect using the same approach of comparison of amplitudes of initial and deformed waviness as was used for elastohydrodynamic effects. This criterion which is developed in Appendix D is:

$$\sigma_t = \frac{3}{2} \frac{(\alpha_s H_s + \alpha_a H_a)}{(h_o - h_i)} \frac{\mu U^2}{h_i^2} \frac{1}{\left(\frac{k_s}{H_s} + \frac{k_a}{H_a}\right)}$$

$\sigma_t \geq 1$ THD effect is significant.

$\sigma_t \ll 1$ THD effect is insignificant.

As with the EHD effect, the THD effect becomes more important as speed, viscosity and axial thicknesses of the seal elements increase and as the average film thickness decreases. Also, as expected, the effect is more important as the coefficient of thermal expansion (α) of the parts increase and as their conductivities (k) decrease.

PRELIMINARY CALCULATIONS FOR REPRESENTATIVE SUBMARINE PROPELLOR SHAFT SEALS

The imput data for two typical high pressure, low speed seals are listed below.

	$5\frac{3}{8}$" Dia. Seal	$17\frac{3}{8}$" Dia. Seal	
r_o	3.625	10.00	in.
r_i	3.250	9.625	in.
μ	1.2×10^{-7}	1.2×10^{-7}	lb/in^2 sec.
N	50 - 200	50 - 200	rpm
p_i	14.7	14.7	psi
p_o	1000 (Assumed)	1000(Assumed)	psi
E_s(seal)	$2\text{-}4 \times 10^6$	$2\text{-}4 \times 10^6$	psi
ν_s	.33	.33	
E_r(rotor)	30×10^6	30×10^6	psi
ν_r	.33	.33	
ρ_f	.0362	.0362	lb/in^3
C_f	1.0	1.0	
K_s	8.7	8.7	B/°F hr ft.
K_r	26.6	26.6	B/°F hr ft.
α_s	4.4×10^{-6}	4.4×10^{-6}	in/in.°F
α_r	5.6×10^{-6}	5.6×10^{-6}	in/in.°F
H_s	.5625	1.0	
$\bar{p}/p_o$	.65	.65	

With this input data, the approximate methods of analysis which have been developed are used to investigate the operation of these seals and indicate which effects are dominating their performance.

These seals have been used extensively in testing and experimental work at MEL. Some representative values of torque and leakage have been obtained for comparison with calculations.

5-3/8" Diameter Seal

Leakage (running)	0.03 gpm
Torque	
200 rpm	10 in-lb.

17-3/8" Diameter Seal

Leakage (running)	0.2 gpm
Torque	
50 rpm	725 in-lb.
200 rpm	375 in-lb.

If it is assumed that all of the frictional torque is caused by shear of the interfacial film, an average film thickness can be derived from measured torque. For the 17-3/8 inch diameter seal the film thicknesses calculated in this way are 2.52 and 19.5 microinches for the 50 rpm and 200 rpm speed conditions respectively. These values are so low that it is not realistic to consider that complete separation of such large surfaces could exist with so small an average film thickness. There must be localized solid to solid contacts and some of the load must be carried in this way. Typical values of coefficient of friction for solid to solid contacts and for hydrodynamic films are 0.3 and 0.005 respectively. If five percent of the load is carried by solid to solid contacts, then approximately 76 percent of the frictional torque would come from these contacts. The average film thicknesses to make up the remainder of the total torque would be 9.4 and 81.3 microinches at 50 rpm and 200 rpm respectively.

If it is assumed that the film thickness is uniform, a film thickness can be calculated from the leakage measurements. Values of 101 and 134 microinches are obtained for the 5-3/8 and 17-3/8 inch diameter seals respectively.

a) Minimum Film Thickness based on a Linear Convergent Profile

$5\frac{3}{8}$" Diameter Seal

Assuming that $(\bar{h}_o - \bar{h}_i) \cong \frac{p_o H_s}{E_s}$ and $p_o = 1000$ psi, then

$$\frac{\Lambda}{\lambda^2} = \frac{6\mu w}{p_o}\left(\frac{r_o - r_i}{p_o H_s} E_s\right)^2$$

$$= \frac{6 \times 1.2 \times 10^{-7} \times 20.9}{1000}\left(\frac{0.375 \times 2 \times 10^6}{1000 \times 0.5625}\right)^2 = 0.0268$$

For $\bar{P}/p_o = 0.65$, $\epsilon_2 = 0.2$ and $\frac{\Lambda}{\lambda^2} < 2$ we obtain λ from Fig. 3

$$\lambda \cong 0.85$$

$$\Lambda \cong 0.85^2 \times 0.0268 = 0.0194$$

$$\bar{h}_i \cong \frac{p_o H_s}{E_s \lambda} = \underline{330 \times 10^{-6}} \text{ in}$$

The computer program also gives a leakage rate

$$Q = 8.647 \cdot \frac{r_m p_o \bar{h}_i^3}{6\mu(r_o - r_i)}$$

$$= 8.647 \cdot \frac{3.6375 \times 1000 \times 3.3^3 \times 10^{-12}}{6 \times 1.2 \times 10^{-7} \times 0.375} = \underline{4 \text{ cu.in/sec. or } 1.04 \text{ gpm}}$$

Similarly, for the $17\frac{3}{8}$" diameter seal

$$\frac{\Lambda}{\lambda^2} = \frac{6 \times 1.2 \times 10^{-7}}{1000}\left(\frac{.375 \times 2 \times 10^6}{1000 \times 1.0}\right)^2 \times 20.9 = 0.00848$$

for $\bar{P}/p_o = 0.65$, $\epsilon_2 = 0.2$

$$\lambda \cong 0.85$$

$$\Lambda \cong 0.00612$$

$$\bar{h}_i \cong \frac{500}{0.85} = \underline{587.5 \times 10^{-6}} \text{ in}$$

$$Q = 8.647 \cdot \frac{10 \times 1000 \times 5.87^3 \times 10^{-12}}{6 \times 1.2 \times 10^{-7}(.375)} = \underline{64.8 \text{ cu.in/sec.}}$$

$$\text{or } \underline{16.8 \text{ gpm}}$$

The linear convergent profile which was assumed in this calculation is very similar to the elastically deformed film profile predicted by the analysis of Nau and Turnbull. It is important to recognize that with the linear convergent profile or the Nau and Turnbull profile there will be no net hydraulic balance force holding the faces of these seals together. Instead, the hydraulic forces will be balanced when the faces are separated by the film thicknesses calculated above and this separation should exist independently of rotation.

The film thicknesses deduced from torque and leakage measurements for these seals are much smaller than those calculated assuming a linear convergent profile. Moreover, the calculation applies when the shaft is stationary and there is an even greater disparity when the experimental behavior under this condition is considered. Leakage is sharply lower when the seal is stationary than it is when running and the starting torque is substantially larger than the running torque. Evidently, the radial film profile of the actual seal differs significantly from the deformed profile obtained using the analysis of Nau and Turnbull also.

b) Elastic Deformation

Equation B24 is used to calculate the radial deformation of the seal ring for a given radial pressure distribution. Figure 7 shows two radial film profiles for the 17-3/8' inch seal assuming a linear pressure distribution and a fully effective bonding surface. The radial seal surface is deformed into a concave profile because of the restriction to axial displacement at the bonding surface. The maximum deformation is found to be approximately 120 microinches.

Obviously, this concave profile will lead to a drastic change in hydraulic balance force in the direction of higher force holding the faces together, and this has been shown in Ref. (8) by Snapp. Of course, the true film shape

in reality must be one which satisfies the elastic and hydrodynamic requirement simultaneously; but it does point out that by including shear effect in the elasticity solution it is possible to explain the small film thicknesses which are indicated by experimental torque and leakage measurements.

Uncertainty over the effects of uneven wear remains. However, the concave deformation profile obtained with inclusion of boundary shear effects in the analysis fits naturally with the rounded edge profile characteristic of these seals after disassembly. This was not true of the deformed profile obtained from the analysis of Nau and Turnbull since in that case the greatest wear would occur in the area of maximum film thickness. That is, given an initially flat surface, the maximum film thickness under pressure would be at the edge adjacent to the high pressure and this is the same area where greatest wear is usually observed.

c) Average Film Temperature

$5\frac{3}{8}$" Diameter Seal

ΔT_f (Average film temperature rise)

$$= \frac{1.75\times10^{4}\cdot 1.2\times10^{-7}\cdot 20.9^{2}\cdot 3.4375^{3}\cdot .375\times10^{4}}{.0362\cdot Q\cdot(\bar{h}_i\times10^{4})}$$

$$= 0.0383/Q\cdot(\bar{h}_i\times10^{4}) \quad {}^{\circ}F$$

$17\frac{3}{8}$" Diameter Seal

$$\Delta T_f = \frac{1.75\times10^{4}\cdot 1.2\times10^{-7}\cdot 20.9^{2}\cdot 9.8125^{2}\cdot .375\times10^{4}}{.0362\times Q\cdot(\bar{h}_i\times10^{4})}$$

$$= 0.8975/Q\cdot(\bar{h}_i\times10^{4}) \quad {}^{\circ}F$$

For the measured values of leakage and assuming a 50 microinch film thickness, the average film temperature rise becomes 2.54 F and 8.95 F for the 5-3/8 and 17-3/8 inch diameter seals respectively.

The temperature distribution within the primary seal elements has been calculated using an available two-dimensional heat transfer program and assuming a uniform heat flux at the faces. The heat flux is determined by assuming a uniform film thickness of 50 microinches and using the input data for the 17-3/8 inch diameter seal. The results are shown in Figure 8 as a temperature map of the primary seal elements.

These results concur with the experimental observation of low temperature rise of th~e seals during operation.

d) Estimate of Elastohydrodynamic Effects

$5\frac{3}{8}$" Diameter Seal

Assuming $\bar{h}_i = 100\ \mu in$

$$\sigma_E = 0.75\,\mu\omega\left(\frac{r_o - r_i}{\bar{h}_i}\right)^2 \frac{H_s}{\bar{h}_i E_s}$$

$$\sigma_E = 0.75 \times 1.2\times10^{-7} \times 20.9 \left(\frac{.325}{10^{-3}}\right)^2 \frac{0.5625}{10^{-3} \times 2\times10^{6}} = 0.0745$$

which indicates that for $\bar{h}_i = 100\ \mu in$, the EHD effect is insignificant. To find the threshold value of the average film thickness at which the EHD effect begins to be significant, we let $\sigma_E = 1$ and $\bar{h}_i = (0745)^{1/3} \times 100 = 27\ \mu in$

$17\frac{3}{8}$" Diameter Seal

for $\bar{h}_i = 100\ \mu$ in

$$\sigma_t = 0.75\,\mu\omega\left(\frac{h_o - h_i}{\bar{h}_i}\right)^2 \frac{H_s}{\bar{h}_i E_s}$$

$$= 0.75 \times 1.2 \times 10^{-7} \times 20.9 \left(\frac{.375}{10^{-6}}\right)^2 \frac{1.0}{10^{-6} \times 2 \times 10^6}$$

$$= 0.132$$

e) Estimate of Thermal-Hydrodynamic Effect

$5\frac{3}{8}$" Diameter Seal

Assuming $\bar{h}_i = 100\ \mu$ in

$$\sigma_t = \frac{3}{2} \frac{(\alpha_s H_s + \alpha_n H_n)}{(h_o - h_i)} \frac{\mu U^2}{\bar{h}_i^2} \frac{1}{\left(\frac{h_s}{H_s} + \frac{h_n}{H_n}\right)}$$

$$= 1.5 \frac{(44 \times .5625 + .56 \times 1.0) \times 10^{-6}}{.375} \cdot \frac{1.2 \times 10^{-7} \times (20.9 \times 3.4375)^2 \times 3600}{10^{-8}\left(\frac{8.7}{.5625} + \frac{26.6}{1.0}\right) \times 778}$$

$$= 0.222$$

Therefore the thermal-hydrodynamic effect is most likely not significant unless the average film thickness falls below the assumed value.

$17\frac{3}{8}$" Diameter Seal

Assuming $\bar{h}_i = 100\ \mu$ in

$$\sigma_t = 1.5 \frac{(44 \times 1.0 + 5.6 \times 1.0) \times 10^{-6} \times 1.2 \times 10^{-7} \times (20.9 \times 9.8125)^2 \times 3600}{.375 \times 10^{-8}\left(8.7/1.0 + 26.6/1.0\right) \times 778} = 2.64$$

The thermal-hydrodynamic effect may be significant for the 17 $\frac{3}{8}$" diameter seals. This conclusion appears to be contradictory to that obtained from the estimate of film temperature rise (part c). This is because the estimate for THD effect considers only conduction of heat into the surfaces and assumes no convection (zero leakage). This assumption is conservative, especially for low speed, high pressure seals.

f) Dynamic Seal Response

According to Equation (8), the response A_n due to the nth harmonic forcing components is

$$A_n = f_n \frac{1}{\left[\left(1 + \frac{k_1}{k_2} - \frac{n^2\omega^2 m}{k_2}\right)^2 + \left(\frac{n\omega c}{k_2}\right)^2\right]^{1/2}}$$

where

$$\frac{1}{k_1} = \frac{1}{k_s} + \frac{AE}{H_s}$$

$$\frac{1}{k_2} = \frac{1}{k_f} + \frac{AE}{H_s}$$

In order to use Figure 3 to calculate the stiffness of the film, we find

$$k_f = -\frac{d}{d\bar{h}_i}(\bar{p}A)$$

Now, $(\bar{h}_o - \bar{h}_i)$ is approximately equal to $\frac{p_o H_s}{E_s}$; therefore, it remains constant with respect to the change of $\bar{h}_i$ and

$$d\bar{h}_i = d\left(\frac{\bar{h}_i}{\bar{h}_o - \bar{h}_i}\right) = d\left(\frac{1}{\lambda}\right)$$

It follows that

$$k_f = -\frac{p_o A}{(\bar{h}_o - \bar{h}_i)} \frac{d(\bar{p}/p_o)}{d(\frac{1}{\lambda})} = \frac{p_o A \lambda^2}{(\bar{h}_o - \bar{h}_i)} \frac{d(\bar{p}/p_o)}{d\lambda}$$

For the 5 $\frac{3}{8}$" diameter navy seals, Figure 3 gives the slope

$$\frac{d(\bar{p}/p_o)}{d\lambda} = 0.135$$

for $\lambda \cong 0.85$ and $\epsilon_2 = 0.4$, $0 < \frac{\Lambda}{\lambda^2} < 5.0$

Using this figure, it is found

$$k_f = \frac{1000 \times 2\pi \times 3.4375 \times .375 \times .85^2}{2.81 \times 10^{-4}} \times .135$$

$$= 2.72 \times 10^6 \quad lb/in.$$

$$\frac{AE}{H_s} = \frac{2\pi \times 3.4375 \times .375 \times 2 \times 10^6}{.5625}$$

$$= 28.9 \times 10^6 \quad lb/in$$

$$k_2 = \frac{1}{\left(\frac{1}{k_f} + \frac{AE}{H_s}\right)} = \frac{10^6}{\left(\frac{1}{2.72} + \frac{1}{28.9}\right)} = 2.45 \times 10^6 \quad lb/in$$

The stiffness of the back-up springs is estimated to be 200 lb/in.; therefore

$$k_1 \cong 200 \quad lb/in$$

Estimating the viscous damping due to the "o" ring to be $C = 1$ and $m = \frac{50}{386} \frac{lb\,sec^2}{in}$

$$\frac{m\omega^2}{k_2} = \frac{438 \times 50}{386 \times 2.45} \times 10^{-6} = 2.32 \times 10^{-5}$$

which is much greater than $\frac{\omega C}{k_2}$, therefore

$$A_m \cong f_m \left(1 + n^2\omega^2 m / k_2\right)$$

for $\frac{A_m}{f_m} = 1.1$, it is found $\underline{n \cong 65.5}$

which means that for a 10% seal response in amplitude, the frequency of the excitation must be something of the order 50 times greater than the rotor frequency.

The similar calculation was made for the 17 $\frac{3}{8}$" diameter seal; it was found

$$k_f = 4.52 \times 10^6 \quad lb/in$$

$$k_2 = 4.125 \times 10^6 \quad lb/in$$

Again assuming $C = 1$ and $m = 200/386 \quad lb\,sec^2/in$

$$\omega^2 m / k_2 = 5.5 \times 10^{-5}$$

for $A_m/f_m = 1.1$, we have $\underline{n \cong 43}$

CORRELATION OF THE ANALYSIS WITH THE EXPERIMENTAL RESULTS OF DENNY (REF. 9)

The approximate methods for seal performance analysis which have been developed are broadly applicable to seals operating over a wide range of speeds, sealed fluid pressures and fluid viscosity. The representative seals which were analyzed in the preceding section operated at the very low speeds, extremely high pressure and low sealed fluid viscosity characteristic of a deep submergence submarine propellor shaft seal. The results for these seals are in substantial agreement with experimental observations. The applicability of the analysis should be investigated further by comparison of results with experimental data for higher speed, moderate pressure seals using higher viscosity fluids. For such a seal the dominant factors in performance are likely to be hydrodynamic and thermal effects instead of radial film shape and pressure induced elastic deformation. Denny[9] presents the most comprehensive body of experimental data for a medium to high speed, moderate pressure seal and therefore his results will be compared with the analysis.

Denny measured the load capacity (relationship between total applied load and face separation) for his seal for several speeds and fluid viscosities. A series of his data points are given in Figure 9 on a plot of $\bar{p}/p_o$ against Λ. The theoretical program for calculation of film pressure for an arbitrary film shape can be used to determine the amplitude of circumferential surface waviness which would be required to generate the measured load capacity. This calculated waviness amplitude can then be compared with the amplitude of the cyclic fluctuation which Denny reports for his film thickness measurements to get an indication of whether hydrodynamic action induced by surface waviness is responsible for the load capacity of his seal.

Since the sealing pressure is relatively low in Denny's cases, it is reasonable to assume that the film is flat radially and has a saddle shape circumferentially. Using this assumption, the theoretical value of $\bar{p}/p_o$ is calculated and plotted against Λ in Figure 9 with the amplitude of the waviness as the parameters.

The table below shows the observed film thicknesses for a range of loads, the corresponding value of Λ and the amplitude of circumferential waviness required to create the experimentally observed load.

$\bar{h}i \times 10^4$	Λ	$\bar{P}/P_o$ Exp. Observed	ϵ_2 Extrapolated from Theoret. Curves	$\epsilon_2 \bar{h}_i$ Amplitude in μ in.
.60	628.0	5.1	0.136	8.15
.70	461.0	2.15	0.078	5.45
.85	312.8	1.15	0.053	4.50
1.00	226.0	.84	0.045	4.50

Denny reports that the amplitude of oscillation in film thickness measurements varied from test to test but that the majority of readings were between 8 and 10 microinches. This agrees closely enough with the calculated amplitudes to support the notion that hydrodynamic effect induced by circumferential waviness could be a primary influence in load capacity of moderate to high speed, moderate pressure seals.

Denny also observed that as the mean film thickness was reduced in steps, a point was reached where the applied load which was supported began to rise sharply above the sealed fluid pressure. That is, there was a film thickness at which hydrodynamic effects rather suddenly became increasingly significant in load support. This is shown by the sharp change in slope of the curves when the shaft was rotating in Figures 5c and 5d of Denny's report which are reproduced as Figure 10 in this report. One possible explanation for the sudden increase in the effectiveness of hydrodynamic load support mechanism at some critical value of film thickness is that the elastohydrodynamic may have become important at that point, thus reinforcing and increasing a small initial circumferential surface waviness. To investigate this possibility our criterion for estimating the importance of the elastohydrodynamic effect was applied. The conditions for the four series of measurements in Figures 5c and 5d of Denny's report are:

Series No.	Speed rpm	Fluid	Applied Pressure-psi	μ reyns	$r_o - r_i$ in	H_s in	E_s psi
1	3000	Tellus 27 Oil	15	3.0×10^{-7}	0.3	0.125	2×10^6
2	500	Tellus 27 Oil	15	4.0×10^{-7}	0.3	0.125	2×10^6
3	3000	Kerosene	15	1.2×10^{-7}	0.3	0.125	2×10^6
4	500	Kerosene	15	1.5×10^{-7}	0.3	0.125	2×10^6

The EHD effect should become significant when $\sigma_E = 1$. The film thickness at which $\sigma_E = 1$ can be expressed as:

$$\bar{h}_i^* \cdot 10^4 = \left[6 \frac{\mu \omega}{\theta} \frac{(r_o - r_i)^2}{E_s} H_s \right]^{1/3}$$

The following table compares the calculated transitional film thicknesses with those at which Denny observed a sharp increase in load capacity:

Series No.	Calculated $\bar{h}_i^*$ microin.	Observed $\bar{h}_i^*$ microin.
1	72.5	80
2	44.0	50
3	54.2	60
4	32.0	28

The close agreement between the experimentally observed and calculated transitional values indicates strongly that the high load capacity observed in practice is associated with the elastohydrodynamic interaction between the fluid and the solid.

CONCLUSIONS

Approximate methods of analysis have been developed to investigate the importance of various aspects of radial face seal performance. These methods have been applied using the operating conditions and design features which are regarded as typical of submarine propeller shaft seals. They have also been applied to explain some of the experimental results of Denny using a higher speed, lower pressure seal. The results lead to several conclusions regarding the most important aspects of the performance of deep submergence propeller shaft seals.

1. The profile of the interfacial film in the radial direction and the most influential factors in its determination are of primary importance in high pressure seals. Simplified elasticity analysis considering only axial compressive deformation of the low modulus primary seal element indicates that there will be no net hydraulic load tending to hold the faces together for a typical propeller shaft seal operating at very high pressure. Instead, the hydraulic forces will be balanced when there is a continuous film separating the faces, even when there is no rotation. Operational experience with this and similar seals clearly rejects this conclusion, thus indicating the inadequacy of that analysis. When the effects of the support structure, including shear at the seal ring-retainer ring boundary, are considered, but still using a simplified type of analysis, a film shape is obtained which is more consistent with experimental observations.

2. At the present time the exact manner in which wear will alter the radial film shape with time is unknown. Some means of considering wear in the analysis of radial film shape and pressure distribution is needed. Conceivably this could be in the form of a relationship between local wear rate and some one or group of parameters in seal operation such as local film thickness, speed or load. Or it may be that further investigation will show that there is an exact pattern of wear which is sufficiently characteristic that it can be used as an initial, undeformed shape in calculations of elastic deformation and film pressure distribution.

3. There is unequivocal evidence that the performance of conventional submarine propeller shaft seals is strongly dependent on whether the shaft is rotating and at what speed. The approximate analysis of the more prominent, and plausible, postulated mechanisms for hydrodynamic pressure generation in face seals indicated that significant pressures can be generated if (a) the mean film thickness is small, below 100 microinches, (b) the circumferential variations in film thickness is of the same order of magnitude as the mean film thickness, and (c) subambient pressures are prevented by occurrence of film rupture. Torque measurements tend to indicate that mean film thicknesses of under 100 microinches are characteristic of submarine propeller shaft seals.

4. Circumferential variations in film thickness may be perpetuated in spite of wear or other attentuating effects by elastohydrodynamic or thermal-hydrodynamic effects. Estimates of the importance of elastohydrodynamic action in large, high pressure, low speed seals indicate that the effect will become significant at mean film thicknesses below 40 or 50 microinches. Estimates of the importance of thermal-hydrodynamic effects indicates that they may be important for film thicknesses of the order of 100 microinches but this assumes that there will be no heat carried away by convection. If leakage rates in the lower range of the measured values reported for the sample seals (.5 gpm for the 17-3/8 inch diameter seal) and mean film thicknesses of 50 microinches or so are assumed, the thermal-hydrodynamic effect will be significant.

5. To investigate the applicability of the analysis developed here to other face seals operating at higher speeds, lower pressures and sealing more viscous fluids, an effort was made to explain some of the features of the behavior of such a seal as observed and reported by Denny[9]. The results indicate that the analysis is applicable to investigation of face seals operating under these conditions also.

REFERENCES

1. Iny, F. H. And Cameron, A. "The Load Carrying Capacity of Rotary Shaft Seals", B.H.R.A. First International Conference on Fluid Sealing, Paper A-2,1961.

2. Whiteman, K. J. "Pressure Generation in Radial Face Seals", B.H.R.A. TN 578, February 1958.

3. Nahavandi, A. and Osterle, M. "The Effect of Vibration on the Load-Carrying Capacity of Parallel Surface Thrust Bearings", ASME Paper 60-LUBS-3, March 1960.

4. Tanner, R. I. "The Reiner Centripetal Effect in Face Seals", B.H.R.A. First International Conference on Fluid Sealing, Paper E1, 1961.

5. Saibel, E. and Lyman, F. A. "A Theoretical Investigation of Leakage Through Rotary Shaft Seals". Report on Contract N 161S-1590-61 to U.S. Naval Engineering Experimental Station, November 1961.

6. Nau, B. S. and Turnbull, D. E. "Some Effects of Elastic Deformation on the Characteristics of Balanced Radial Face Seals", B.H.R.A. First International Conference on Fluid Sealing, Paper D3, 1961.

7. Fisher, M. J. "An Analysis of the Deformation of the Balanced Ring in High-Pressure Radial-Face Seals", B.H.R.A. First International Conference on Fluid Sealing, Paper D4, 1961.

8. Snapp, R. B. "An Analytical Study of Thin Fluid Films in Face-Type Shaft Seals", U.S. Naval Experiment Station, NP/9430(851), July 1962.

9. Denny, D. F. "Some Measurements of Fluid Pressures Between Plane Parallel Thrust Surfaces with Special Reference to the Balancing of Radial Race Seals", B.H.R.A., Report No. RR-163, January 1959.

10. Jagger, E. T. "Study of Lubrication of Synthetic Rubber Rotary Shaft Seals". Inst. Mech. Engr. Conference on Lubrication and Wear, October 1957.

11. Timoshenko, S. and Goodier, J. N. Theory of Elasticity, McGraw-Hill Book Company, Second Edition, 1951, p. 370.

APPENDIX A - Analysis of Pressure for an Arbitrary Film Shape

As a result of elastic or thermal distortions or because of uneven wear, the seal ring and rotor surfaces may deform into a convergent or divergent section radially and a wavy shape circumferentially. The equation governing the pressure for a given film shape is the Reynolds equation for the incompressible fluid in cylindrical coordinates. Referring to the coordinates shown in Figure 2, the Reynolds equation is

$$\frac{1}{r^2}\frac{\partial}{\partial\theta}\left(\frac{h^3}{\mu}\frac{\partial p}{\partial\theta}\right)+\frac{1}{r}\frac{\partial}{\partial r}\left(\frac{rh^3}{\mu}\frac{\partial p}{\partial r}\right)=\frac{6U}{r}\frac{\partial h}{\partial\theta}+12\frac{\partial h}{\partial t} \tag{A1}$$

Introducing

$P = p/p_r$

p_r = a reference pressure (in this report p_o is used in the reference pressure).

$\xi = \frac{r-r_i}{r_o-r_i}$

$H = h/\bar{h}_i$

$\bar{h}_i$ = circumferential mean film thickness at inner radius

$\tau = \omega t$

Equation (2) becomes

$$\left(\frac{r_o-r_i}{r}\right)^2\frac{\partial}{\partial\theta}\left(H^3\frac{\partial P}{\partial\theta}\right)+\left(\frac{r_o-r_i}{r}\right)H^3\frac{\partial P}{\partial\xi}+\frac{\partial}{\partial\xi}\left(H^3\frac{\partial P}{\partial\xi}\right)$$
$$=\frac{6\mu\omega}{p_r}\left(\frac{r_o-r_i}{\bar{h}_i}\right)^2\left(\frac{\partial H}{\partial\theta}+2\frac{\partial H}{\partial\tau}\right) \tag{A2}$$

For most of the seals considered in this report,

$$r \gg r_o-r_i$$

therefore, equation (A2) can be further simplified by ignoring the first two terms on the right hand side and it becomes the well-known short bearing equation

$$\frac{d}{d\xi}\left(H^3\frac{dP}{d\xi}\right)=\Lambda\left(\frac{\partial H}{\partial\theta}+2\frac{\partial H}{\partial\tau}\right) \tag{A3}$$

where

$$\Lambda=\frac{6\mu\omega}{p_r}\left(\frac{r_o-r_i}{\bar{h}_i}\right)^2$$

Three forms of the film thickness function will be considered; they are:

1. $H = H(r,\theta)$ (A4)
2. $H = H(r,\theta-\omega t)$ (A5)
3. $H = H(r,\theta+\omega t)$ (A6)

Variation of the shape of the film between the stator and rotor can be caused by rigid body motions of the rotor and stator such as axial oscillation, rocking, elastic or thermal elastic deformations, and initial deviation from flatness. In the case where the film variations are primarily caused by the initial imperfection or stationary deformation of the stator, equation (4) is applicable; on the other hand, if most of the warping or deformation occurs in the rotor, then equation (5) should be used. Equation (5) is also applicable for the case where the deformation in the stator is not stationary but exists as a fixed shape wave travelling around at the same speed and direction as that of the rotor. Equation (6) represents a possible case where a wave exists in the stator travelling at the rotor frequency but in the opposite direction - a backward synchronous wave.

The substitution of (4) through (6) to the right hand side of equation (3) gives the following forms respectively:

$$\Lambda \frac{\partial H(r,\theta)}{\partial \theta}$$

$$-\Lambda \frac{\partial H(r,\theta-\omega t)}{\partial(\theta-\omega t)}$$

and

$$-3\Lambda \frac{\partial H(r,\theta+\omega t)}{\partial(\theta+\omega t)}$$

It is seen that the same method for integration of the pressure can be used for all three cases.

Proceeding on with the integration of equation (3), we have

$$P(\xi) = \Lambda I_1(\xi) + C_1 I_0(\xi) + C_2 \quad \text{(A7)}$$

where

$$I_1(\xi) = \int_0^{\xi} \frac{1}{H^3} f(\eta)\, d\eta \tag{A8}$$

$$f(\xi) = \int_0^{\xi} \frac{\partial H}{\partial \theta}\, d\eta \tag{A9}$$

$$I_2(\xi) = \int_0^{\xi} \frac{1}{H^3}\, d\eta \tag{A10}$$

Using the boundary conditions,

$$\begin{aligned} P &= P_i/p_a \quad \text{at} \quad \xi = 0 \\ P &= P_o/p_a \quad \text{at} \quad \xi = 1 \end{aligned} \tag{A11}$$

the pressure distribution becomes

$$P - P_i = \Lambda\, I_1(\xi) + \left[\frac{P_o - P_i - \Lambda\, I_1(1)}{I_2(1)} \right] I_2(\xi) \tag{A12}$$

The film thickness is represented by a set of continuous functions of θ at a set of discrete values of ξ_k as follows:

$$H_k(\theta) = C_k + \sum_{m=1}^{M} a_{km} \cos m\theta + b_{km} \sin m\theta \tag{A13}$$

for

$$k = 1, \ldots\ldots K$$

Using Simpson's rule for the numerical integration and allowing no subambient pressures to appear in the film, a computer program was written to calculate the pressure distributions in the film.

APPENDIX B - Analysis of Elastic Deformations

Approximate Analysis of Rotor Elastic Deformation

A schematic representation of a typical seal subjected to an arbitrarily distributed pressure is shown on page 11 of the main text. If it is assumed that deformation due to bending is negligible and that the pressure is distributed over the annular sealing surface and is independent of the radius, the normal deformation of the rotor due to normal pressure acting on the face can be calculated by using the classical half-space solution.

Using the foregoing simplifications, the circumferential normal displacement can be estimated by

$$H(\theta) = \int_0^{2\pi} \frac{\bar{q}(\alpha)}{\left|\sin\frac{\alpha-\theta}{2}\right|}\, d\alpha \qquad \text{(B1)}$$

where

$$H(\theta) = \frac{2\pi E h}{(1-\nu^2)\, p_r (r_o - r_i)}$$

$$\bar{q}(\alpha) = \frac{1}{p_r (r_o - r_i)} \int_{r_i}^{r_o} p\, dr$$

p_r a reference pressure

The singularity occurring at $\theta = \alpha$ in the integrand can be overcome by putting Eq. (B1) into the following form:

$$\int_0^{2\pi} \frac{\bar{q}(\alpha)}{\left|\sin\frac{\alpha-\theta}{2}\right|}\, d\alpha = \int_0^{\theta-\Delta\alpha} \frac{\bar{q}(\alpha)}{\left|\sin\frac{(\alpha-\theta)}{2}\right|}\, d\alpha + \int_{\theta+\Delta\alpha}^{2\pi} \frac{\bar{q}(\alpha)}{\left|\sin\frac{\alpha-\theta}{2}\right|}\, d\alpha + f(\theta) \qquad \text{(B2)}$$

where f (θ) represents the deformation contributed by the pressure between $-\Delta\theta$ and $\Delta\theta$ and it is approximated by

$$f(\theta) = 7.42\, m \left(\frac{2R\Delta\theta}{\Delta r}\right)^{1/4} \bar{q}(\theta) \qquad \text{(B3)}$$

The value m can be taken from p. 370 of Ref. (11).

Approximate Analysis of Stator Elastic Deformation Considering Effects of Retainer Ring

If it is assumed that the circumferential hoop stress in the carbon ring is much smaller than the radial compressive stress, the axial strain can be expressed as

$$\epsilon_z \cong \frac{\sigma_z}{E_s} - \nu \frac{\sigma_r}{E_s} \tag{B4}$$

The normal displacement therefore becomes

$$\omega_z(\theta, r) = \int \epsilon_z(z, \theta, r)\, dz + C_1 \tag{B5}$$

The distribution of the radial stresses, σ_r, in the seal ring is influenced greatly by the elastic deformation fo the adjacent steel retainer ring. An approximate analysis of this retainer ring using the theory of cylindrical shells is obtained as follows:

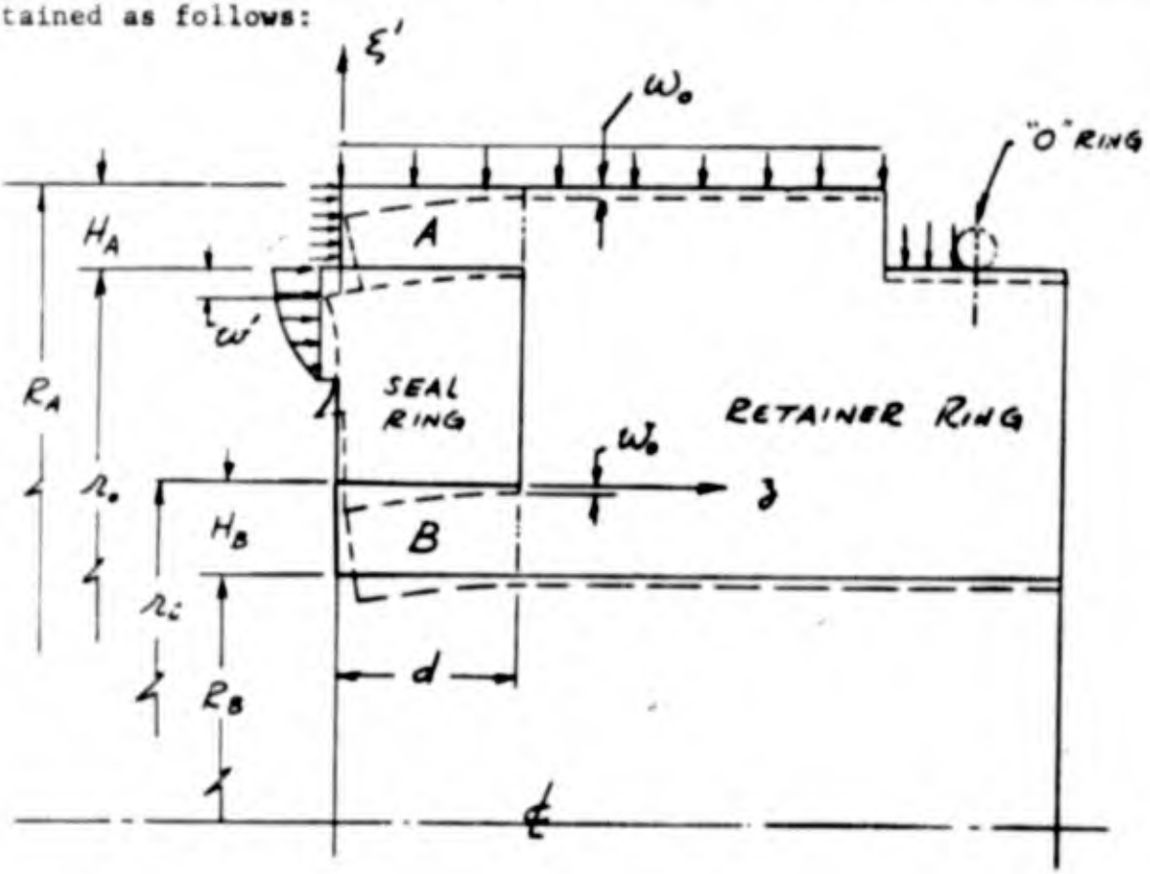

The dotted shape represents the deformed shape of the seal and retainer ring under the external pressure. The forces acting on the ring section A are shown below.

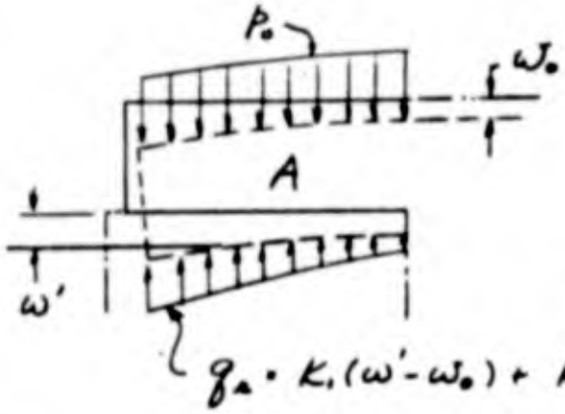

Assuming that the inner radius of the section "A" is resting on an elastic foundation having an effective spring stiffness K_1, the equation governing the radial deformation of ring section "A" is

$$\frac{d^4\omega'}{dz^4} + 4\beta'\omega' = \frac{P_o}{D} - \frac{K_1(\omega' - \omega_o) + K_2\omega_o}{D} \tag{B6}$$

where

$$\beta'^4 = \frac{3(1-\nu^2)}{R_A^2 H_A^2}$$
$$D = \frac{E H_A^3}{12(1-\nu^2)} \tag{B7}$$

Let $\omega = \omega' - \omega_o$, then Equation (B6) becomes

$$\frac{d^4\omega}{dz^4} + 4\beta\omega = \frac{P_o}{D} - 4\beta'^4\omega_o - \frac{K_2\omega_o}{D} \tag{B8}$$

where

$$\beta^4 = \beta'^4 + \frac{K_1}{4D} \tag{B9}$$

and following the notation used by Snapp, the general solution of Equation (B8) becomes

$$\omega = A\sin\beta z\cosh\beta z + B\sin\beta z\cosh\beta z + L\cos\beta z\sinh\beta z + G\cos\beta z\cosh\beta z + \left[\frac{P_o - K_2\omega_o}{4\beta^4 D} - \left(\frac{\beta'}{\beta}\right)^4\omega_o\right] \tag{B10}$$

Using the following boundary conditions

$$z = d\,,\quad \omega = 0\,,\quad \frac{d\omega}{dz} = 0$$
$$z = 0\,,\quad M_z = 0\,,\quad \frac{d^2\omega}{dz^2} = 0 \tag{B11}$$
$$z = 0\,,\quad F_z = 0\,,\quad \frac{d^3\omega}{dz^3} = 0$$

we have the particular solution

$$w = L(\sin\beta z\cosh\beta z + \cos\beta z\sinh\beta z) + G\cos\beta z\cosh\beta z + \left[\frac{p_o - K_1 w_o}{4\beta^4 D} - \left(\frac{\beta'}{\beta}\right)^4 w_o\right] \tag{B12}$$

where

$$L = \left[\frac{p_o - K_2 w_o}{4\beta^4 D} - \left(\frac{\beta'}{\beta}\right)^4 w_o\right]\left[\frac{\cos\beta d\sinh\beta d - \sin\beta d\cosh\beta d}{\cosh^2\beta d + \cos^2\beta d}\right] \tag{B13}$$

$$G = -\left[\frac{p_o - K_2 w_o}{4\beta^4 D} - \left(\frac{\beta'}{\beta}\right)^4 w_o\right]\frac{2\cos\beta d\cosh\beta d}{\cosh^2\beta d + \cos^2\beta d} \tag{B14}$$

For $z = 0$

$$w|_{z=0} = \left[\frac{p_o - K_2 w_o}{4\beta^4 D} - \left(\frac{\beta'}{\beta}\right)^4 w_o\right]\left[1 - \frac{2\cos\beta d\cosh\beta d}{\cosh^2\beta d + \cos^2\beta d}\right] \tag{B15}$$

The term $K_2 w_o$ is the uniform compressive stress required to deform the seal ring through a constant radial displacement w_o and

$$K_2 = \frac{E_s(r_o - r_i)}{\left(\frac{r_o + r_i}{2}\right)^2} \tag{B16}$$

where E_s is the modulus of the elasticity of the seal ring. The constant radial displacement can be approximated by

$$w_o = \frac{p_o\left(\frac{R_A + R_B}{2}\right)^2}{E(R_A - R_B)} \tag{B17}$$

The stiffness K_1 can be approximated by

$$\frac{1}{K_1} = \frac{1}{K_3} + \frac{1}{K_4} \tag{B18}$$

where K_3 is the radial stiffness of the seal

$$K_3 = \frac{E_s}{(r_o - r_i)} \tag{B19}$$

and K_4 is the stiffness of the ring section "B" which can be approximated by using Equation (B9) and expressed as

$$K_4 = \left(\frac{E H_B}{R_B^2}\right)\frac{1}{\left[1 - \frac{2\cos\beta_1 d\cosh\beta_1 d}{\cosh^2\beta_1 d + \cos^2\beta_1 d}\right]} \tag{B20}$$

where

$$\beta_1^4 = \frac{3(1-\nu^2)}{R_B^2 H_B^2} \tag{B21}$$

Using the following dimensionless coordinates

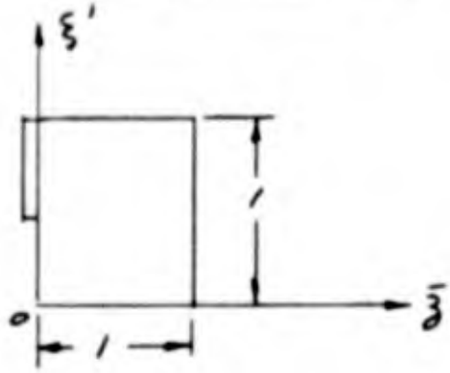

$$\xi' = \frac{r - r_i}{r_o - r_i}$$

$$\bar{z} = z/d$$

the radial stress thus can be approximated by the following expression:

$$\sigma_r(\xi', \bar{z}) = -(K_1\omega + \xi' K_2 \omega_o) \tag{B22}$$

If the bonding surface is assumed to carry no surface shear traction, then the axial stress can be approximated by

$$\sigma_z(\xi', \bar{z}) = -p(\xi') \tag{B23}$$

which is the relation used by Nau Turnbull and Snapp. However, this is not a realistic assumption since the bonding agent is known to be impervious to high hydrostatic fluid pressure and therefore must be able to withstand considerable shear traction. In order to allow this shear effect, a weighting function is used to enforce the axial strain to be zero at $\xi' = o$ and $\xi' = 1$. Using this weighting function, the axial strain becomes

$$\epsilon_z = \frac{\sigma_z}{E_s} - \nu\frac{\sigma_r}{E_s} = \frac{1}{E_s}\left[-p(\xi') + \nu K_1\omega + \xi'\nu K_2\omega_o\right]\left\{1 - \bar{z}^{[a - b\ln 2|\xi' - \frac{1}{2}|]}\right\} \tag{B24}$$

The exponent "a" measures the effectiveness of the shear carrying capacity of the bond. The cases for $a = o$, $1 > a > o$, and $a = 1$, imply the bond is fully effective, partially effective and ineffective.

The exponent "b" measures the penetration of the shear effect into the core; a small value of "b" implies deep penetration of the shear effect and a large value of "b" means shallow penetration, which means the shear effect is mostly concentrated at the boundary.

Once the axial strain distribution is known, the normal displacement can be calculated from Equation (B5).

APPENDIX C - Analysis of the Significance of Elastohydrodynamic Effects in the Circumferential Direction

Assuming the film profile is constant in the radial direction and is represented by

$$H = 1 + \epsilon_2 \cos 2\theta$$

then the steady state Reynolds equation becomes

$$\frac{d^2P}{d\xi^2} = \frac{\Lambda}{H^3}\frac{\partial H}{\partial \theta} \tag{C1}$$

Integrating (C1) and using the following boundary conditions

$$\xi = 0 \quad , \quad P = 0$$
$$\xi = 1 \quad , \quad P = 0$$

we have

$$P = \frac{\Lambda}{H^3}\frac{\partial H}{\partial \theta}\xi(\xi - 1) \tag{C2}$$

and

$$P_{max.}\Big|_{\substack{\xi=\frac{1}{2} \\ \theta=\frac{3\pi}{4}}} = \frac{\Lambda \epsilon_2}{4} \tag{C3}$$

or

$$P_{max.} = 6\mu\omega\left(\frac{R_0 - R_i}{\bar{R}_i}\right)^2 \frac{\epsilon_2}{4} \qquad \text{AND} \qquad P_{min} = 0$$

Assuming that the local elastic deformation is directly proportional to the local pressure, then the amplitude of the deformed waviness is

$$h_a = \frac{h_{max.} - h_{min}}{2} \simeq \left(\frac{P_{max} - P_{min}}{2}\right)\frac{H_s}{E_s} \tag{C4}$$

$$= \frac{6\mu\omega\epsilon_2}{8}\left(\frac{R_0 - R_i}{\bar{R}_i}\right)^2 \frac{H_s}{E_s}$$

If $h_a \geq \epsilon_2 \bar{h}_i$ then the elastohydrodynamic effect is significant and

if $h_a \ll \epsilon_2 \bar{h}_i$ then the elastohydrodynamic effect is insignificant.

Defining

$$\sigma_E = \frac{6\mu\omega}{\delta}\left(\frac{r_o - r_i}{\bar{h}_i}\right)^2 \frac{H_s}{\bar{h}_i E_s}$$ we have

$$\sigma_E \geq 1 \qquad \text{EHD effects significant}$$

$$\sigma_E \ll 1 \qquad \text{EHD effects insignificant} \qquad \text{(C5)}$$

APPENDIX D - Analysis of the Significance of Thermal-Hydrodyanamic Effects in the Circumferential Direction

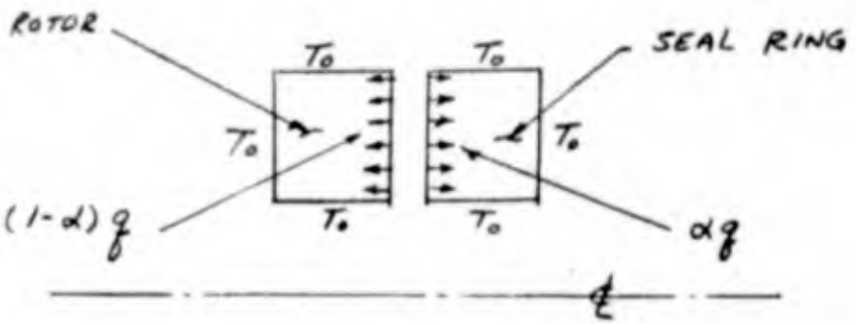

Assuming the temperature is parabolic in the radial direction and linear in the axial direction, the temperature in the seal ring can be represented by

$$T_s = 4(T_{s_{max}} - T_o)\xi(1-\xi)(1-\bar{\zeta}) \tag{D1}$$

where $\bar{z}$ is an axial coordinate with the positive direction downward.

Similarily, the temperature in the rotor can be expressed as

$$T_r = 4(T_{r_{max}} - T_o)\xi(1-\xi)(1-\bar{\zeta}) \tag{D2}$$

where $\bar{z}$ now is an axial coordinate with the positive direction upward.

Let αq and $(1-\alpha)q$ be the heat conducted away per unit circumferential length by the seal ring and rotor respectively.

$$\alpha q = -\int_0^1 k_s \frac{r_o - r_i}{H_s} \frac{\partial T_s}{\partial \bar{\zeta}} d\xi$$

$$(1-\alpha)q = -\int_0^1 k_r \frac{r_o - r_i}{H_r} \frac{\partial T_r}{\partial \bar{\zeta}} d\xi \tag{D3}$$

Integrating (D3) we have

$$\alpha q = \frac{k_s(r_o - r_i)}{H_s} \frac{2}{3}(T_{s_{max}} - T_o)$$

$$(1-\alpha)q = \frac{k_r(r_o - r_i)}{H_r} \frac{2}{3}(T_{r_{max}} - T_o) \tag{D4}$$

Assuming $T_{s_{max.}} = T_{r_{max.}} = T_{max}$, we have

$$q = \frac{2}{3}(r_o - r_i)\left(\frac{k_s}{H_s} + \frac{k_r}{H_r}\right)(T_{max.} - T_o) \tag{D5}$$

or

$$T_{max.} - T_o = \frac{3q}{2(r_o - r_i)\left(\frac{k_s}{H_s} + \frac{k_r}{H_r}\right)} \tag{D6}$$

Now

$$q = \mu\left(\frac{U}{\bar{h}_i}\right)^2 \frac{r_o - r_i}{H} \tag{D7}$$

where

$$H = 1 + \epsilon_2 \cos 2\theta$$

The maximum thermal growth of the seal ring and rotor is

$$\begin{aligned} w_t &= (\alpha_s H_s + \alpha_r H_r)(T_{max.} - T_o)\int_o^1 (1-\bar{z})\, d\bar{z} \\ &= (\alpha_s H_s + \alpha_r H_r)(T_{max} - T_o)/2 \\ &= \frac{3}{4}(\alpha_s H_s + \alpha_r H_r)\, q \left[(r_o - r_i)\left(\frac{k_s}{H_s} + \frac{k_r}{H_r}\right)\right]^{-1} \\ &= \frac{3}{4}(\alpha_s H_s + \alpha_r H_r)\frac{\mu U^2}{\bar{h}_i}\left[(r_o - r_i)\left(\frac{k_s}{H_s} + \frac{k_r}{H_r}\right)(1 + \epsilon_2 \cos 2\theta)\right]^{-1} \end{aligned} \tag{D8}$$

The amplitude of the waviness due to the thermal growth is

$$\frac{1}{2}\left(w_t\big|_{\theta=\frac{\pi}{2}} - w_t\big|_{\theta=0}\right) \tag{D9}$$

The following criteria will be used to determine the significance of the thermal-hydrodynamic effect:

$$\frac{1}{2}\left(w_t\big|_{\theta=\frac{\pi}{2}} - w_t\big|_{\theta=0}\right) \geq \epsilon_2 \bar{h}_i \tag{D10}$$

The THD effect is significant and

$$\frac{1}{2}\left(w_t\big|_{\theta=\frac{\pi}{2}} - w_t\big|_{\theta=0}\right) \ll \epsilon_2 \bar{h}_i$$

it is insignificant when is small,

$$(1 + \epsilon_2 \cos 2\theta)^{-1} \approx 1 - \epsilon_2 \cos 2\theta$$

It follows

$$\frac{1}{2}(\omega_c|_{\theta=\frac{\pi}{8}} - \omega_c|_{\theta=0}) = \frac{3}{4} \frac{(\alpha_s H_s + \alpha_n H_n)}{r_0 - r_i} \frac{\mu U^2}{R_c} \frac{2\epsilon_2}{\left(\frac{\alpha_s}{H_s} + \frac{\alpha_n}{H_n}\right)} \quad \text{(D11)}$$

The final criteria for the THD effect can be written as

$$\sigma_t = \frac{3}{2} \frac{(\alpha_s H_s + \alpha_n H_n)}{(r_0 - r_i)} \frac{\mu U^2}{R_i^2} \frac{1}{\left(\frac{\alpha_s}{H_s} + \frac{\alpha_n}{H_n}\right)} \geq 1$$ THD effect is significant

$$\sigma_t \ll 1$$ THD effect is insignificant.

NOMENCLATURE

$a_{k,m}$	Fourier coefficient for the film thickness function
A_n	Amplitude Response
$b_{k,m}$	Fourier coefficient for the film thickness function
C	Constant used with the non-symmetrical parabolic profile
C_f	Specific heat of the fluid
C_k	Coefficients for the radial film variation
d	Depth of the seal
D	$EH_A^3/12\ (1-\nu^2)$
E	Modulus of elasticity of the rotor material
E_s	Modulus of elasticity of the seal material
f_n	Amplitude of the exciting motion
F_r	See (B8)
G	See (B14)
h	Film thickness
$\bar{h}_o$	Average film thickness at outer radius
h_a	Amplitude of deformed waviness
$\bar{h}_i$	Average film thickness at inner radius
h_i^*	Transitional film thickness
h_{max}	Maximum radial film thickness
h_{min}	Minimum radial film thickness
H	$h/\bar{h}_i$
H_A	See Figure on p. 36
H_B	See Figure on p. 36
H_r	Depth of the rotor

H_s	Depth of the seal
I_1	See Def. (A8)
I_2	See Def. (A10)
k	Index, see Def. (A13)
k_1	Equivalent spring stiffness
k_2	Equivalent spring stiffness
k_f	Equivalent spring stiffness
k_r	Thermal conductivity of the rotor
k_s	Equivalent spring stiffness, also thermal conductivity of the seal
K	Thermal conductivity
K_1	See (B18)
K_2	See (B16)
K_3	See (B19)
K_4	See (B20)
L	See Equation (B13)
m	See (B3) , also used as mass of the seal
M_z	See (B11)
n	Frequency of the exciting motion
N	Rotational speed of the seal
p	Pressure in the seal interface
p_o	Pressure at outer radius
$\bar{p}$	P/p_r
p_{max}	Maximum pressure
p_{min}	Minimum pressure
p_r	A reference pressure, (in this work, $p_r = p_o$)
P	$= p/p_r$

P_o	p_o/p_r
P_i	p_i/p_r
P_{max}	p_{max}/p_r
P_{min}	p_{min}/p_r
$\bar{q}$	$\frac{1}{p_r(r_o-r_i)}\int_{r_i}^{r_o} p\,dr$
Q	Leakage factor
r	Radius of the seal ring
r_o	Outer radius of the seal ring
r_i	Inner radius of the seal ring
r_m	Mean radius of the seal ring
R_A	See Figure on p. 36
R_B	See Figure on p. 36
s	Seal response motion
t	Time corrdinate
T	Temperature of the solid or fluid
T_o	Initial temperature
ΔT_f	Temperature rise
T_r	Temperature of the rotor
T_s	Temperature of the seal
U	Mean velocity of the seal
w'	See Figure on p. 36
w_o	Radial displacement
w_t	Thermal displacement
z	Axial coordinate
$\bar{z}$	z/d

α See Equation (B2), also used as coefficient of thermal expansion

α_r Coefficient of expansion of the rotor

α_s Coefficient of expansion of the seal

β $\left[(\beta')^4 + \frac{K_1}{4D}\right]^{1/4}$

β' $3(1 - \nu^2)/R_A^2 H_A^2$

ϵ_z Axial Strain

ϵ Amplitude of the circumferential waviness

ϵ_2 Amplitude of the second harmonic waviness

η Dummy variable of ξ

θ Angular coordinate

λ $(\bar{h}_o - \bar{h}_i)/\bar{h}_i$

Λ $= \frac{6\mu\omega}{p_o}\left(\frac{r_o - r_i}{\bar{h}_i}\right)^2$

μ Viscosity of the fluid

ν Poisson's ratio

ν_r Poisson's ratio of the rotor

ν_s Poisson's ratio of the seal

ξ $(r - r_i)/(r_o - r_i)$

ξ' See Figure on p. 36

ρ_f Density of the fluid

σ_E Factor determining the inportance of EHD effect

σ_r Radial stress

σ_t Factor determining the importance of THD effect

σ_z Axial stress

τ ωt

ω Angular speed of the seal

β_1 $3(1-\nu^2)/R_0^2 H_0^2$

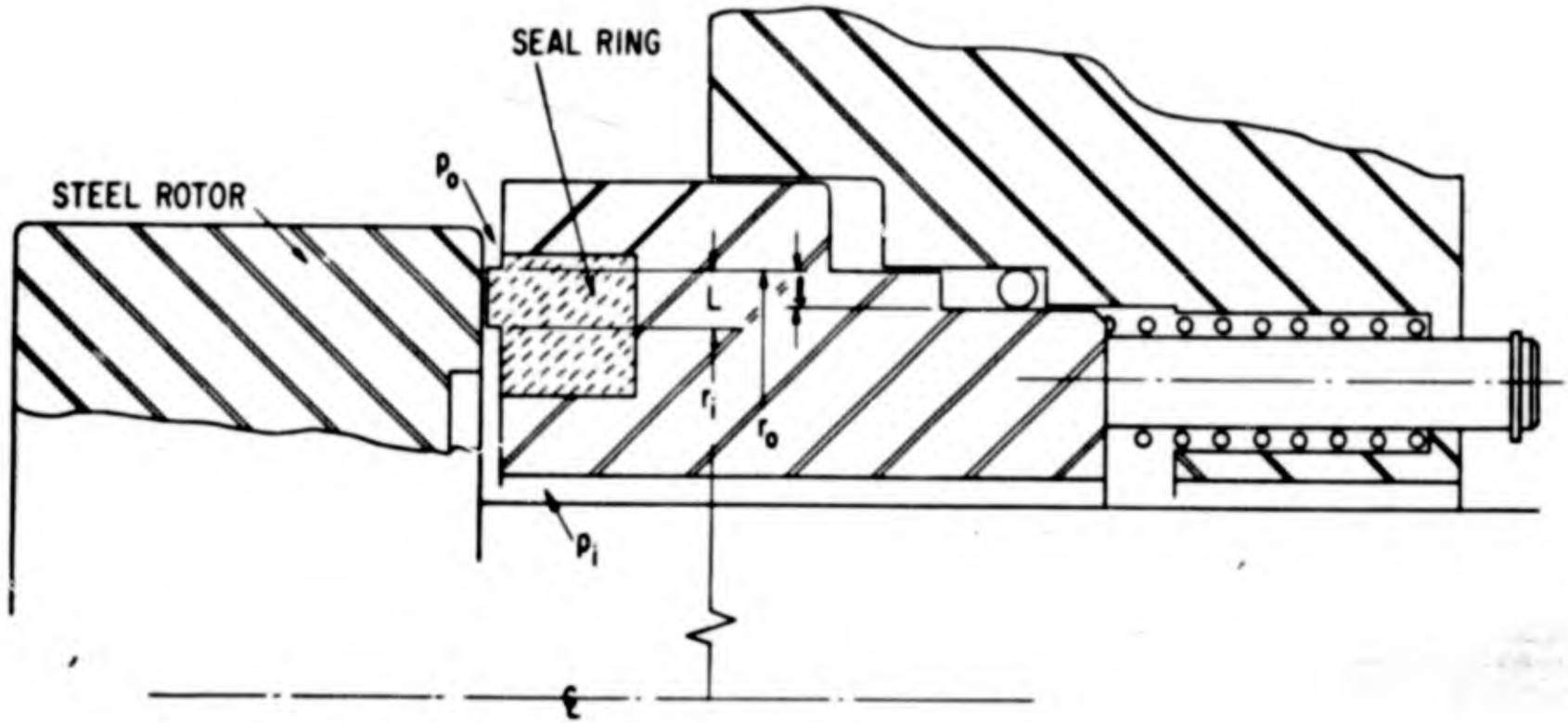

Fig. 1 Schematic of a Representative Face Seal

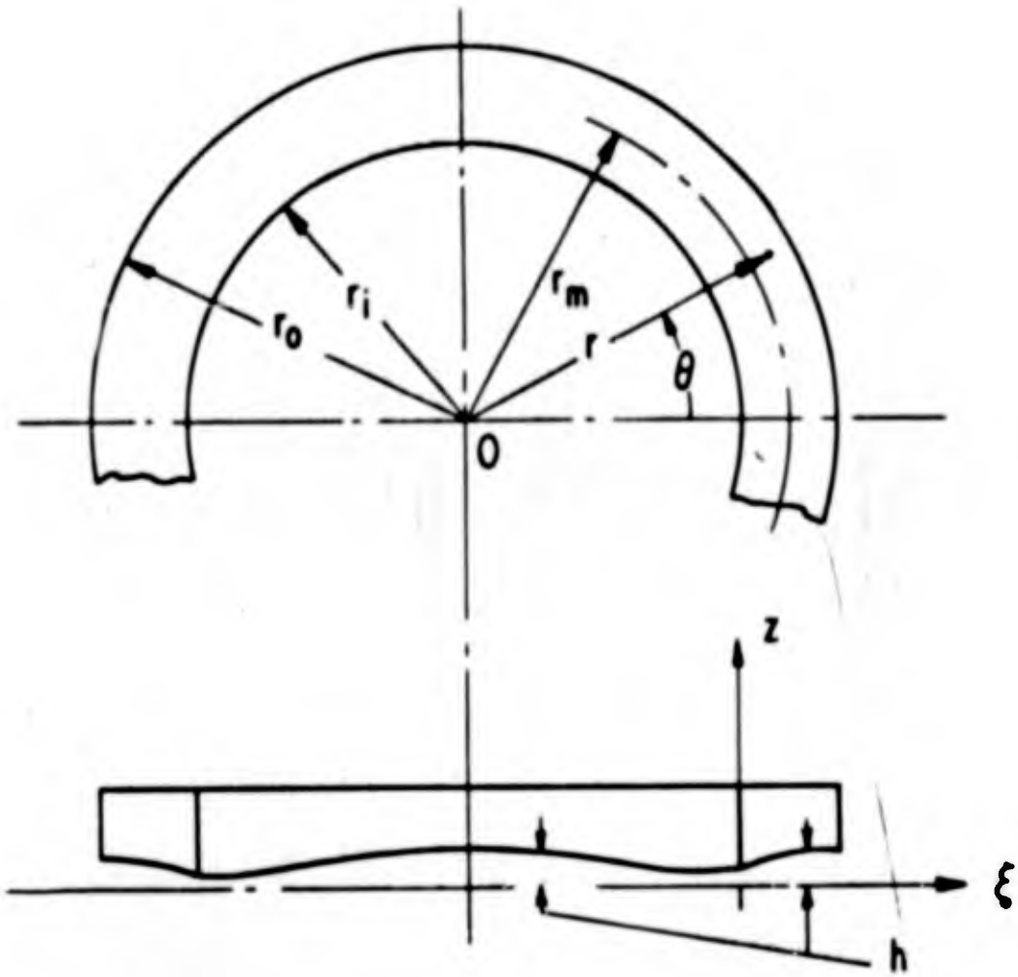

Fig. 2 Coordinates of a Face Seal

BLANK PAGE

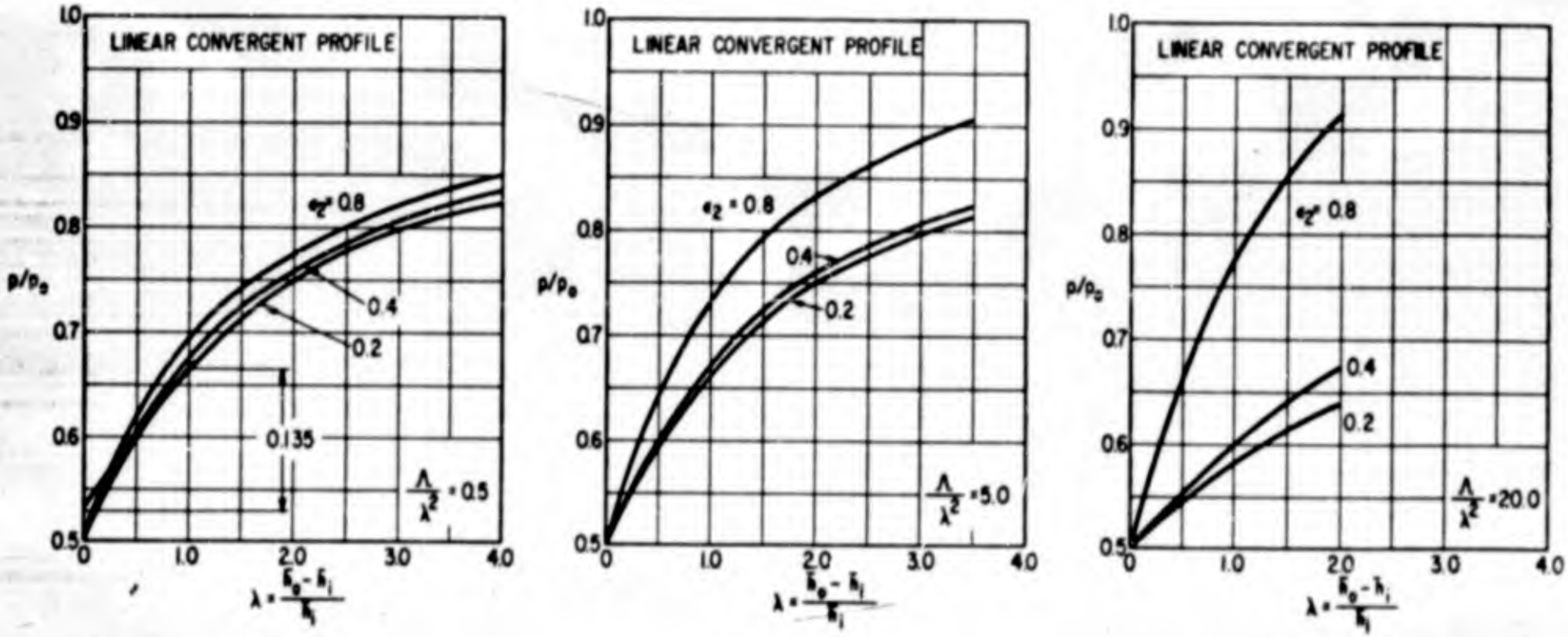

Fig. 3 Load Capacity for Linear Convergent Radial Film Shape

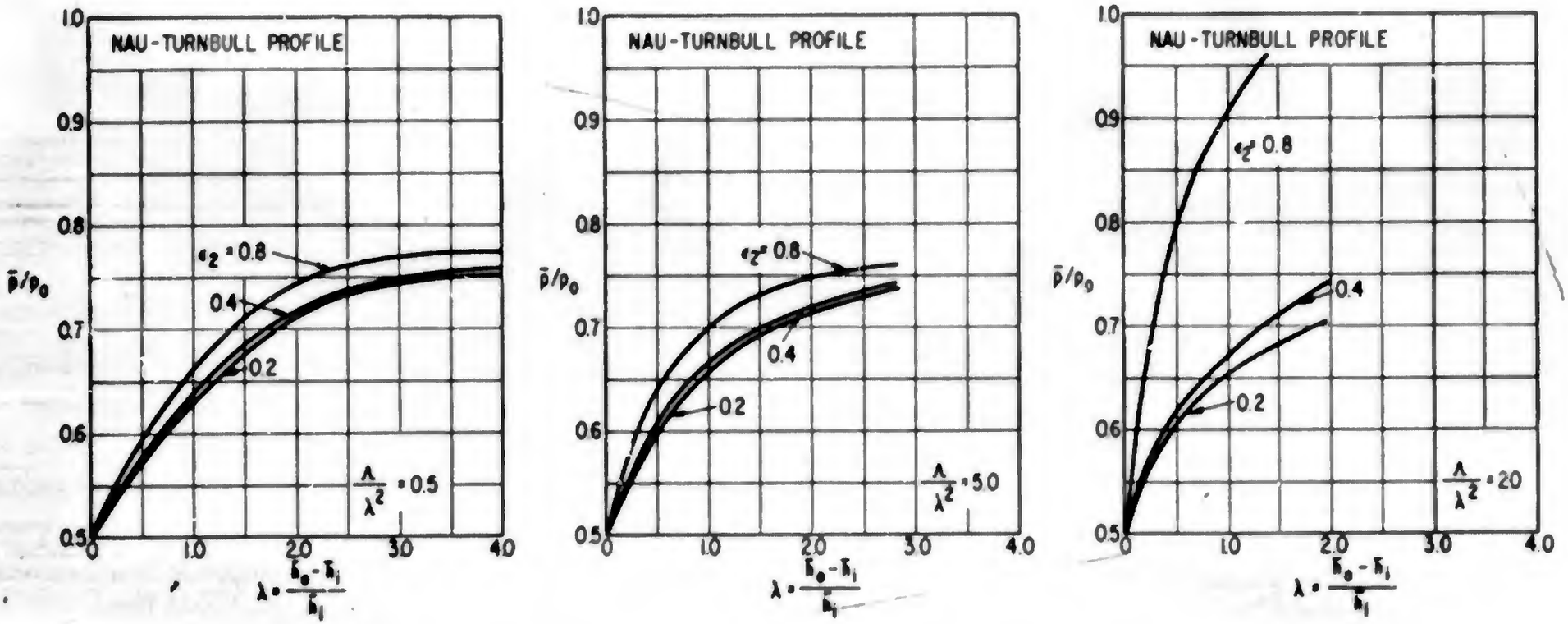

Fig. 4 Load Capacity for Radial Film Shape Determined by Analysis of Nau and Turnbull (Ref. 6)

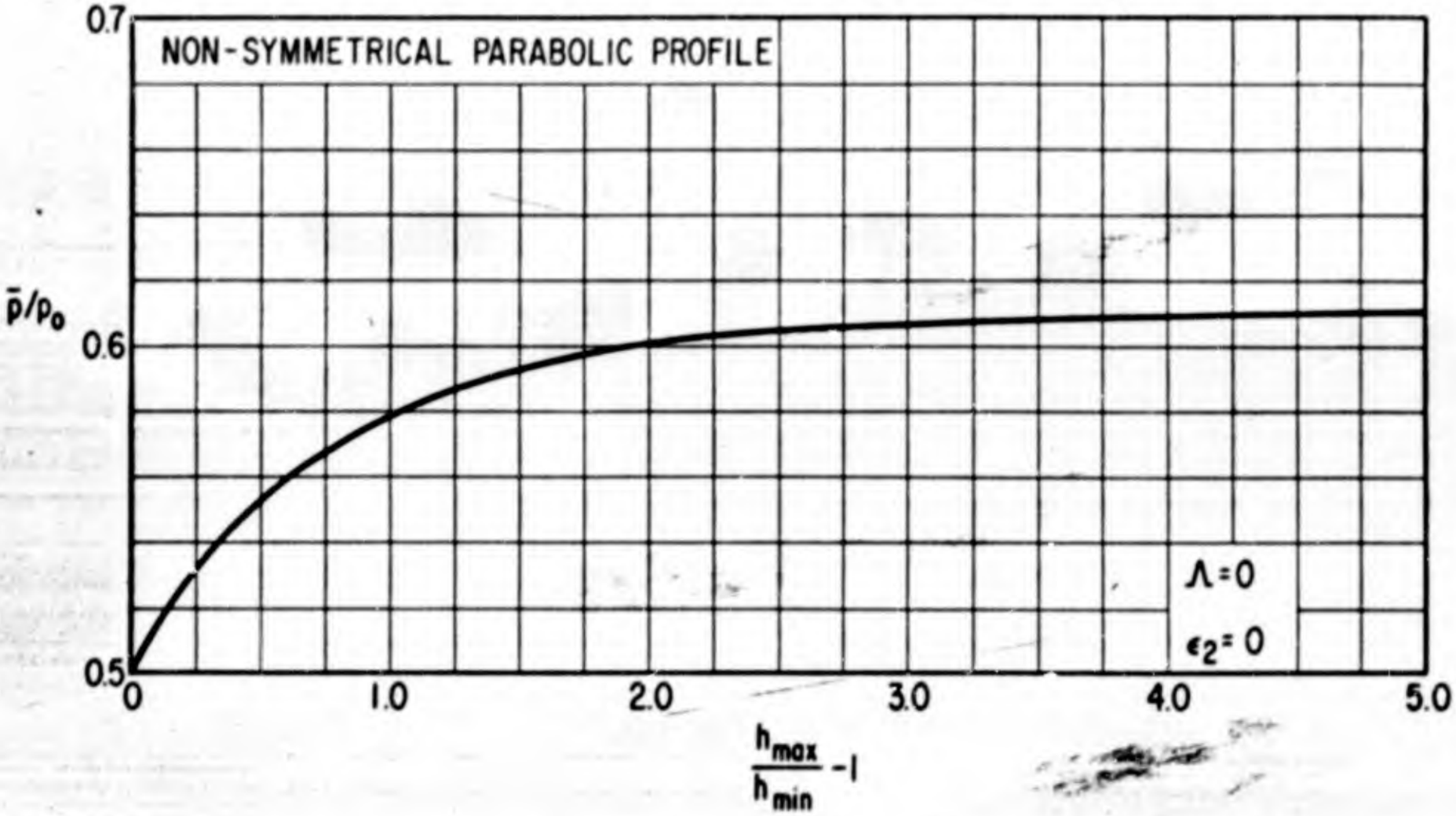

Fig. 5 Load Capacity for a Non-Symmetrical Parabolic Radial Film Shape

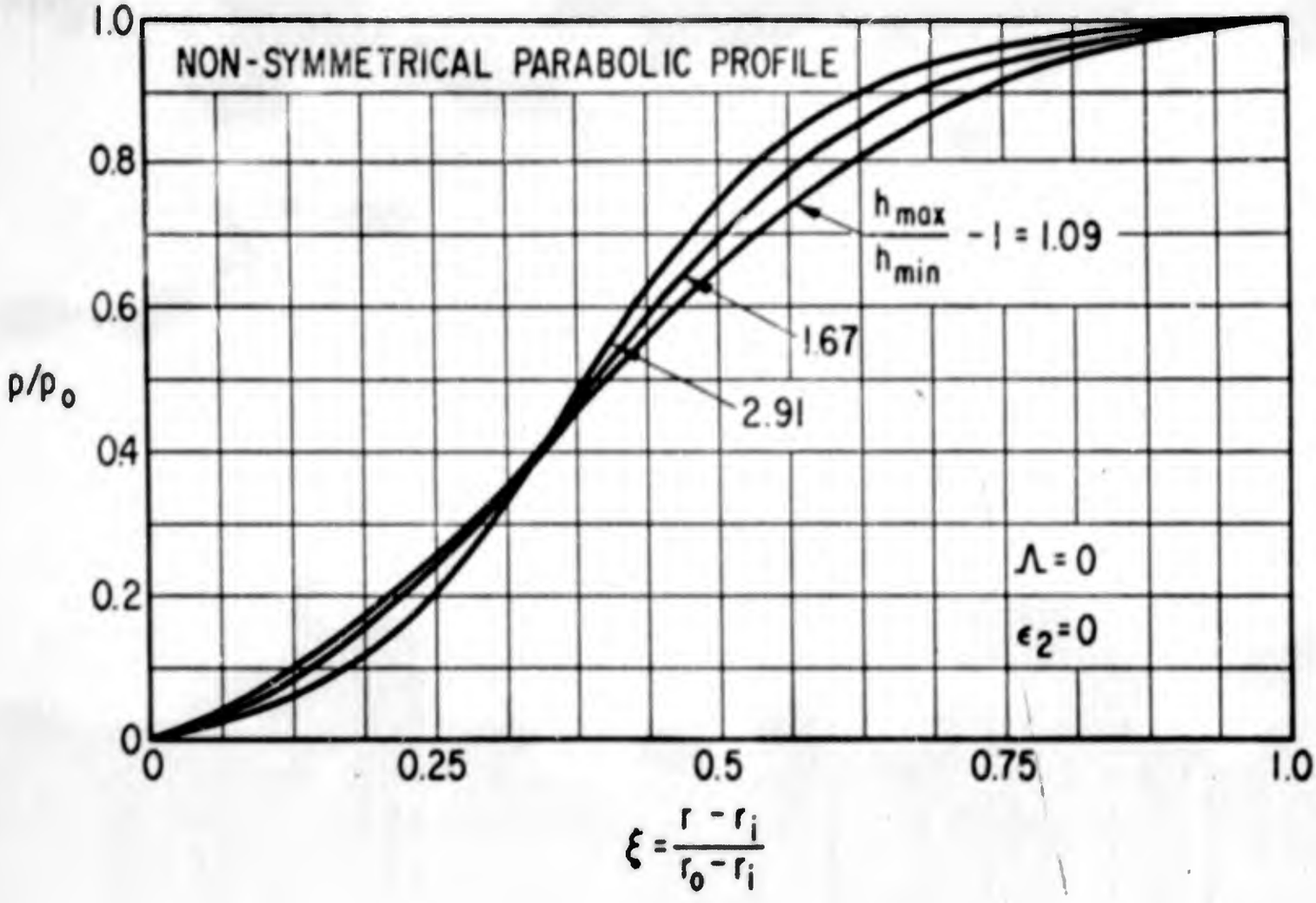

Fig. 6 Radial Film Pressure Distribution — Non-Symmetrical Parabolic Profile

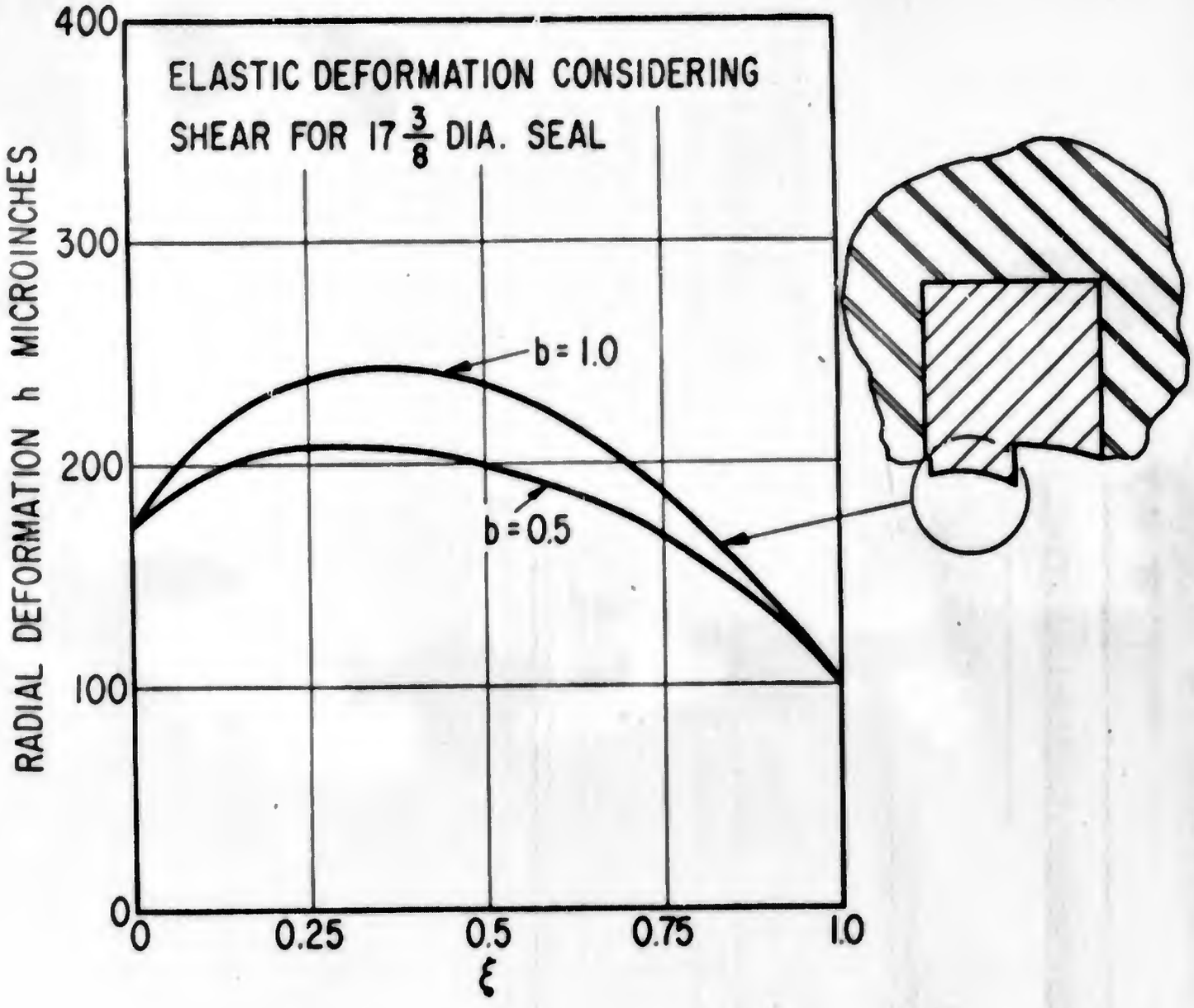

Fig. 7 Approximate Radial Film Shape with Elastic Deformation for 17-3/8 inch Diameter Seal

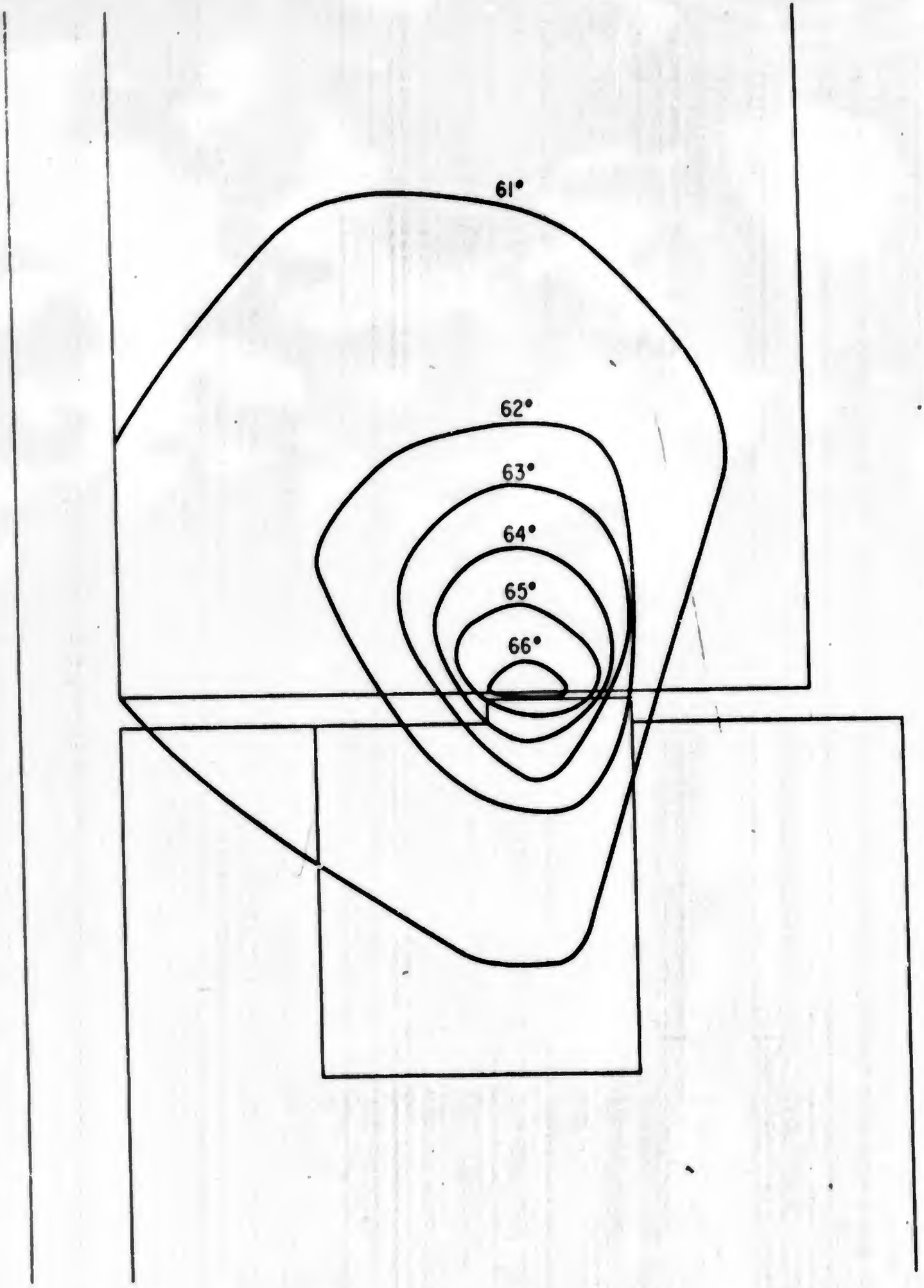

Fig. 8 Temperature Map for 17-3/8 inch Diameter Face Seal

BLANK PAGE

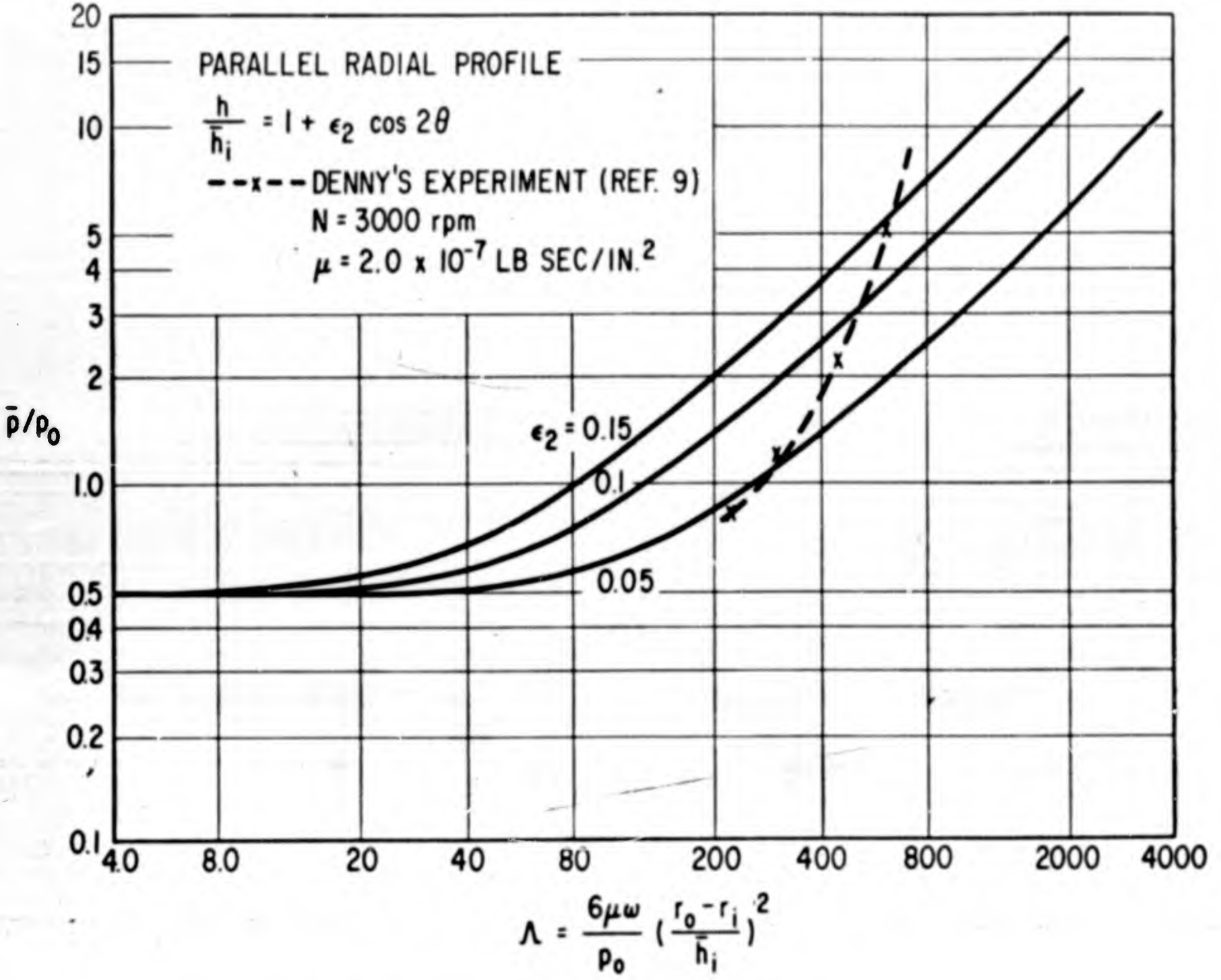

Fig. 9 Load Capacity Curves for Parallel Radial Profile

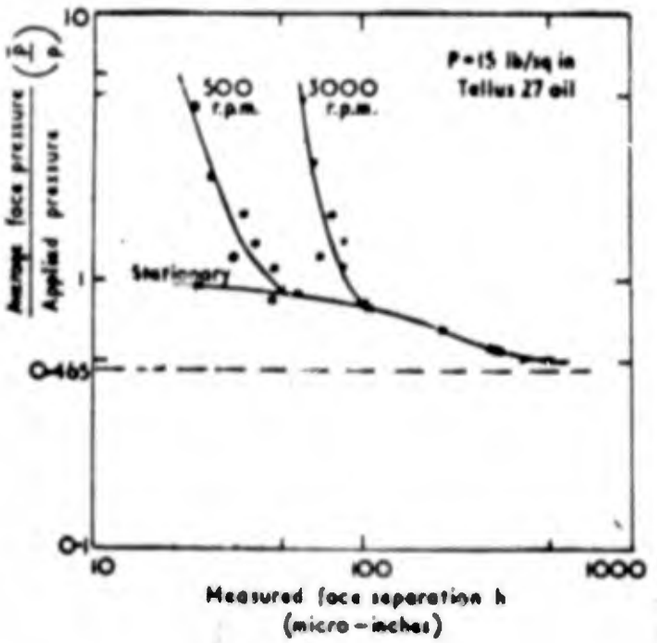

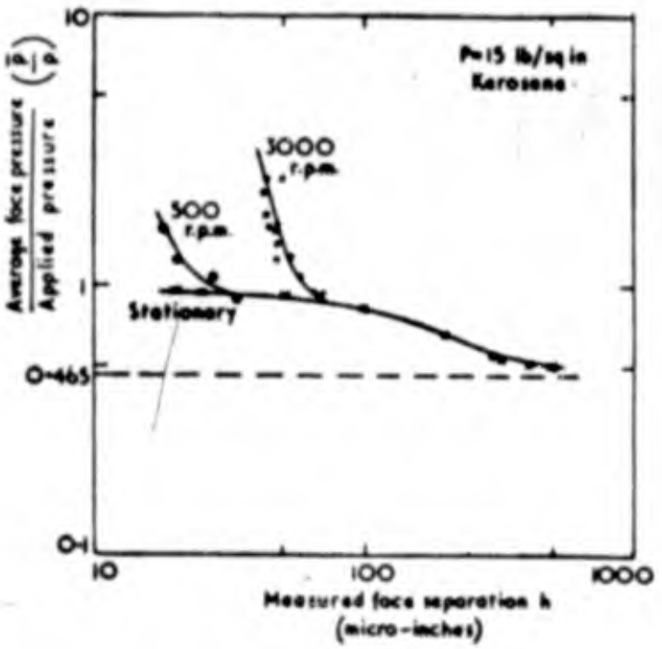

Figure 10

RELATION BETWEEN FACE PRESSURE AND FACE SEPARATION

Courtesy of D. F. Denny (Reference 9)